

Concealing Backdoor Model Updates in Federated Learning by Trigger-Optimized Data Poisoning

Yujie Zhang
Duke University
yujie.zhang396@duke.edu

Neil Gong
Duke University
neil.gong@duke.edu

Michael K. Reiter
Duke University
michael.reiter@duke.edu

Abstract

Federated Learning (FL) is a decentralized machine learning method that enables participants to collaboratively train a model without sharing their private data. Despite its privacy and scalability benefits, FL is susceptible to backdoor attacks, where adversaries poison the local training data of a subset of clients using a backdoor trigger, aiming to make the aggregated model produce malicious results when the same backdoor condition is met by an inference-time input. Existing backdoor attacks in FL suffer from common deficiencies: fixed trigger patterns and reliance on the assistance of model poisoning. State-of-the-art defenses based on analyzing clients’ model updates exhibit a good defense performance on these attacks because of the significant divergence between malicious and benign client model updates. To effectively conceal malicious model updates among benign ones, we propose DPOT, a backdoor attack strategy in FL that dynamically constructs backdoor objectives by optimizing a backdoor trigger, making backdoor data have minimal effect on model updates. We provide theoretical justifications for DPOT’s attacking principle and display experimental results showing that DPOT, via only a *data-poisoning* attack, effectively undermines state-of-the-art defenses and outperforms existing backdoor attack techniques on various datasets.

1 Introduction

Federated Learning (FL) is a decentralized machine-learning approach that has gained widespread attention for its ability to address various challenges. Unlike traditional centralized model training, FL enables model updates to be computed locally on distributed devices, offering enhanced data privacy, reduced communication overhead, and scalability for a large number of clients. In each round of FL, a central server distributes a global model to participating clients, each of whom independently trains the model on their local data, and their model updates are aggregated by the server for updating the global model.

Despite its advantages, FL has been proven susceptible to backdoor attacks [1]. Backdoor attacks in federated learning involve adversaries inducing the local models of a subset of clients to learn backdoor information carried by triggers and strategically integrating these backdoored local models into the global model. Ultimately, the global model will generate the adversary-desired result when the same trigger conditions are met. In this work, we term clients manipulated by adversaries during local training as *malicious clients*, and those unaffected as *benign clients*.

Existing backdoor attacks in FL present two common deficiencies. First, the patterns of backdoor triggers are pre-defined by the attacker and remain unchanged throughout the entire attack process [1, 39, 35, 14]. Consequently, the optimization objective brought by backdoored data (backdoor objective) is static and incoherent with the optimization objective of main-task data (benign objective), resulting in distinct differences in model updates after training. These malicious clients’ model updates are therefore easily canceled out by robust aggregations [1, 46, 14]. Second, many approaches rely on model-poisoning techniques to enhance the effectiveness of backdoor attacks. Implementing model-poisoning attacks requires attackers to change the training procedures of a certain number of genuine clients (e.g., at least 20% of all clients [2, 8, 37]) to make their local training algorithms different from other clients. However, achieving this condition is challenging, as advanced defense mechanisms [29] have introduced Trusted Execution Environments (TEEs) to ensure the secure execution of client-side training, making it harder to adopt suspicious modifications to the training procedure.

Existing defenses against backdoor attacks in FL (see more details in Section 2.4) rely on a hypothesis that backdoor attacks will always cause the updating direction of a model to deviate from its original benign objective, because the backdoor objectives defined by backdoored data cannot be achieved within the original direction. However, the capabilities of backdoor attacks are not limited to this hypothesis. To counter this hypothesis, adversaries can align the updating directions of a model with respect to backdoor and benign objectives by

strategically adjusting the backdoor objective. Applying this idea to FL, if the injection of backdoored data has minimal effect to the updates of a client’s model, then detecting this client as malicious becomes challenging for defenses based on analyzing clients’ model updates.

In this work, we propose **Data Poisoning with Optimized Trigger (DPOT)**, a backdoor attack on FL that dynamically constructs the backdoor objective to continuously minimize the divergence between clients’ model updates in the backdoored states and the non-attacked states. We construct the backdoor objective by optimizing the backdoor trigger that is used to poison malicious clients’ local data. Without any assistance of model-poisoning techniques, malicious clients can effectively conceal their model updates among benign clients’ model updates by simply executing a normal training process on their poisoned local data, and render state-of-the-art defenses ineffective in mitigating our backdoor attack.

The optimization of the backdoor trigger in each round is independent and specific to the current round’s global model. The objective of this optimization is to generate a trigger such that the current round’s global model exhibits minimal loss on backdoored data having this trigger. Once the global model becomes optimal for the backdoored data, further training on the backdoored data will result in only minor model updates to the current state of global model within a limited number of local training epochs. Therefore, when a malicious client’s local dataset is partially poisoned by the optimized trigger while the rest remains benign, the model updates produced by training on the local data will be dominated by benign model updates. We provide both theoretical and experimental justifications for the sufficiency of trigger optimization in minimizing the difference between a malicious client’s model updates in the backdoored state and the non-attacked state.

In order to enhance the practicality of our attack, we limited the trigger size to a reasonable level, ensuring it cannot obscure essential details of the original data. To meet this constraint, we developed two algorithms to separately optimize trigger pixels’ placements and values. To the best of our knowledge, we are the first to generate an optimized trigger with free shape and placement while specifying its exact size.

We evaluated DPOT on four image data sets (FashionMNIST, FEMNIST, CIFAR10, and Tiny ImageNet) and four model architectures including ResNet and VGGNet. We assessed the attack effectiveness of DPOT under a variety of defense conditions, testing it against 10 defense strategies that are based on analyzing clients’ model updates — these include Median [42], Trimmed Mean [42], RobustLR [27], Robust Federated Aggregation (RFA) [28], FLAIR [33], FLCert [6], FLAME [26],

FoolsGold [12], Multi-Krum [3], and FRL [25] — along with one defense strategy that uses client-side adversarial training to recover the global model: Flip [45]. We compared DPOT attack with three state-of-the-art data-poisoning backdoor attacks that employ fixed-pattern triggers, distributed fixed-pattern triggers (DBA [39]), and partially optimized triggers (A3FL [44]), respectively. Using a small number of malicious clients (5% of the total), DPOT outperformed existing data-poisoning backdoor attacks in effectively undermining defenses without affecting the main-task performance of the FL system.

In summary, our contributions are as follows:

- We propose a novel backdoor attack mechanism, DPOT, in FL that effectively conceals malicious client’s model updates among those of benign clients by dynamically adjusting backdoor objectives, and demonstrate that existing defenses focusing on analyzing clients’ model updates are inadequate.
- We dynamically construct the backdoor objective solely by optimizing the backdoor trigger and injecting it to clients’ data (a.k.a. data-poisoning), without relying on additional assistance from model-poisoning techniques.
- We offer both theoretical and experimental justifications for the adequacy of our trigger optimization in reducing the disparity between model updates in the backdoored state and the non-attacked state.
- We develop algorithms to optimize a trigger, allowing for flexibility in its shape, placement, and values, while precisely constraining its size.
- We extensively evaluate our attack on four benchmark datasets, showing that DPOT achieves better attack effectiveness than three advanced data-poisoning backdoor attacks in compromising 11 state-of-the-art defenses in FL.

2 Related Work

2.1 Federated Learning (FL)

The Federated Learning [23] (FL) training process involves four main steps: 1) **Model Distribution**: A central server distributes the most recent global model to the participating clients. 2) **Local Training**: Each client independently trains the global model on its local training dataset and obtains a local model. 3) **Model Updates**: Each client calculates the parameter-wise difference between its local model and the global model, referred to as model updates, and then sends them to the central server. 4) **Aggregation**: The central server aggregates clients’ model updates to create a new global model. This entire process, consisting of step 1 to 4, constitutes a global round. The FL system repeats these

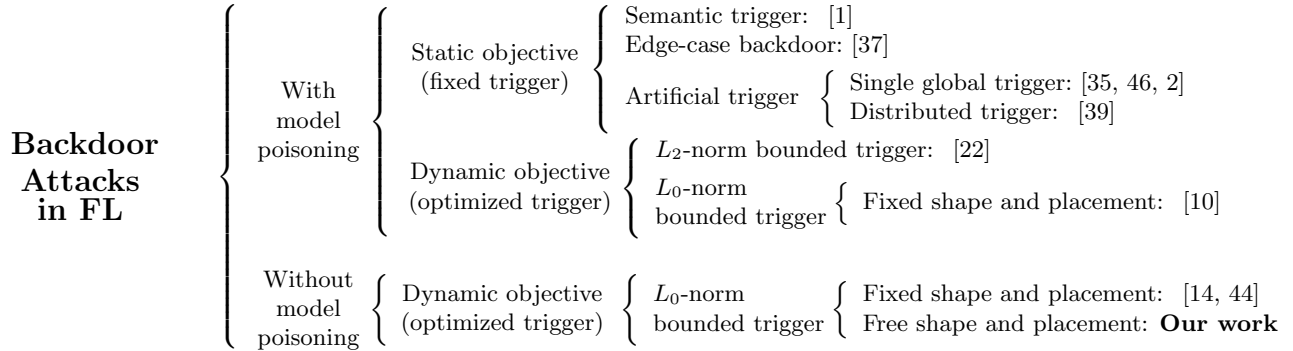


Figure 1: An overview of related works on backdoor attacks in FL.

steps for a certain number of rounds to obtain a final version of the global model.

2.2 Backdoor Attack

Backdoor attack in machine learning is a security vulnerability where an adversary manipulates a model’s behavior by making it learn some trigger information, causing the model to produce erroneous results when trigger conditions are met. Meanwhile, the backdoor attack also ensures that the model maintains normal performance on benign data to evade abnormal detection. In image classification tasks, a backdoor attack aims to manipulate a model so that it classifies any image containing a specific pixel-pattern trigger into a label chosen by the attacker [7, 15, 18, 20, 41, 36, 21].

2.3 Backdoor Attacks in FL

FL is easily suffered from backdoor attacks. As training data are privately held by clients, the security of data is hard to track or protect. Adversaries can inject backdoors into the global model simply by compromising a few vulnerable client devices and poisoning their data with backdoor triggers. To date, many variations of backdoor attacks targeting FL have emerged, and we summarize those specific to image classification tasks in Figure 1.

With model poisoning v.s. Without model poisoning:

The foundation of backdoor attacks in FL is through *data poisoning* - attackers embed backdoor triggers into the local training data of certain clients and change the ground-truth labels of the infected data to malicious labels. As a result, clients’ local models trained on the poisoned data will be backdoored, and consequently, the global model that aggregates these backdoored models will also be backdoored.

A standalone data poisoning is found challenging to succeed when employing some types of triggers. Therefore, many works introduce model poisoning to assist

backdoor attacks in FL. *Model poisoning* aims to either directly manipulate clients’ model updates or indirectly achieve this by changing their local training algorithms. Three main approaches in model poisoning were widely adopted in existing attacks: 1) Scaling based [1, 35, 39, 14]. Attackers amplify malicious model updates generated from backdoored models before clients send them to the server. These malicious updates can overpower the aggregation results, causing the global model to quickly incorporate backdoors. However, this approach is vulnerable to defenses that exclude outlier model updates from the aggregation. 2) Constraint based [1, 22]. Attackers change clients’ local training algorithms by adding extra constraints to their loss functions, giving backdoored models specific characteristics, such as being less distinguishable from benign models. 3) Projection based [46, 2, 37, 10]. Attackers constrain backdoor implementation to bounded model parameters: by clipping parameter values or using Projected Gradient Descent, backdoor models are L_2 -norm bounded to a chosen model state; by selectively updating a subset of parameters, they are L_0 -norm bounded to a chosen state.

Model poisoning requires attackers to modify certain clients’ local training procedures. However, with the introduction of Trusted Execution Environments (TEEs) by state-of-the-art defense mechanisms [29], client-side execution for training can be authenticated and secure, thus increasing the difficulty of conducting model poisoning. In contrast, data poisoning is easier to conduct and harder to prevent since clients may collect their local data from open resources where attackers can also get access to and make modifications. For example, autonomous driving vehicles collect their data on road traffic signage [40] from real world, and attackers can easily place stickers on traffic signage objects to inject backdoor trigger information. Hence, we consider backdoor attacks that do not involve model poisoning to be more advanced than those that do.

Static objective v.s. Dynamic objective:

If a backdoor attack has a specified and unchanging objective that is independent to the training system’s status, we refer to this as a *static objective*. For instance, Semantic trigger as backdoor [1] aims to associate certain features from input that is unrelated to the main training tasks with an attacker-chosen output, causing the model to make incorrect predictions on those inputs; Edge-case backdoor [37] selects data that share certain commonalities but are from the tail end of the input data distribution as the backdoored input, causing the model to mispredict them; Artificial trigger as backdoor [35, 46, 2, 39] embeds a few pixels forming a specific artificial pattern into the input, leading the model to mispredict any input containing this pixel pattern. In FL, since the static objectives of backdoor attacks are inconsistent with the optimization objectives defined by the main-task data, malicious models will exhibit distinct differences in their model updates compared to benign models, making them easy to detect.

In contrast to a static objective, a backdoor attack that adjusts its objective based on the training system’s status is referred to as having a *dynamic objective*. By adjusting its objective, a backdoor attack is expected to achieve greater effectiveness. Several approaches have been proposed in recent attack studies to attempt to accomplish this. For example, Model-dependent attack [14] and F3BA [10] optimized the trigger pattern based on a hypothesis that maximizing the activation of certain neurons in the backdoored local model can enhance the attack’s persistence on the global model, which is however lack of theoretical evidence and proof-of-concept codes; A3FL [44] optimized triggers specifically for a corner case in FL training, where the global model is directly trained to unlearn the trigger, but the effectiveness of A3FL triggers in more general FL training scenarios remains unaddressed.

L_2 -norm bounded optimized trigger v.s. L_0 -norm bounded optimized trigger:

A critical consideration in designing backdoor triggers is ensuring their stealthiness when applied to input data, resulting in a substantial disparity between human perception and the backdoored model’s interpretation. Existing dynamic objective attacks achieve this by constraining the optimized triggers’ L_2 -norm or L_0 -norm bounds.

An L_2 -norm bound on a trigger or perturbation means that the total magnitude of the changes introduced by the backdoor is limited. This makes the perturbation subtle, ensuring it doesn’t drastically alter the input data. For example, CerP [22] generates optimized perturbations of the same size as a data point for each round and adds them to clients’ local data to induce their local models learn to misclassify the perturbed data to

a specified target label.

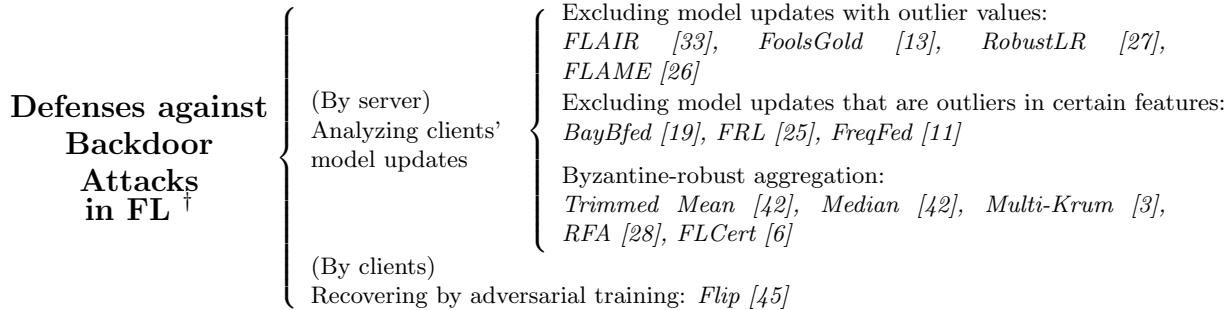
An L_0 -norm bound restricts the number of components (e.g., pixels in an image) that can be altered by the trigger. This constraint ensures that the trigger is sparse, meaning it only affects a small portion of an input data. For example, optimized triggers in Model-dependent attack [14], F3BA [10], and A3FL [44] all consist of a small number of pixels arranged in a square shape and are placed in a fixed corner location on the data to poison.

An L_2 -norm bounded trigger is less practical for real-world data poisoning because it spreads changes across many pixels, requiring the attacker to access and alter a figure’s values before it is physically printed for use. Additionally, these small perturbations are easily disrupted by data preprocessing techniques that filter out unnecessary noise. In contrast, an L_0 -norm bounded trigger is easier to apply to any data (e.g., a sticker on an image) due to its stable shape, consistent values, and compact size. However, existing works in optimizing L_0 -norm bounded triggers are limited by fixing their shapes and placements and only updating triggers’ values, which fails to fully leverage the potential of optimized triggers for attacking FL.

2.4 Defenses against Backdoor Attacks in FL

In this work, we focus on discussing defenses that adhere to the fundamental privacy-preserving principles of FL introduced by McMahan, et al [23] - clients’ private data are kept local, and their model updates are not shared with any entities other than the server. We summarize the related defense works in figure 2. For a discussion on additional defenses with varying privacy-preserving properties, please refer to the Appendices A.2.

In existing defenses, the server and clients are the two subjects commonly considered for implementing defense strategies. For clients as the defense subject, the global model of each round is the input they receive from the FL system. Flip [45] proposed using trigger inversion on the global model and adversarial training on local models to mitigate the impact of the backdoor trigger, which is a defense strategy implemented by benign clients. However, Flip’s effectiveness against optimized triggers remains unaddressed. Optimized triggers are more challenging to recover than fixed ones due to their variability across different rounds. For the server as the defense subject, clients’ model updates are the input that the server receives from the FL system. Numerous studies have proposed defenses against backdoor attacks by analyzing clients’ model updates, which can be further classified into three categories, as discussed below.



[†] In this work, we only discuss defenses that adhere to the fundamental privacy-preserving principles of FL [23] - clients' private data are kept local, and their model updates are not shared with any entities other than the server.

Figure 2: An overview of related works on defenses against backdoor attacks in FL.

Excluding model updates with outlier values: Some existing works believed that a malicious client's model updates will directly exhibit significant difference in values from those of benign clients, therefore excluding model updates with outlier values can mitigate the effects of backdoor attacks. *FLAME* [26] and *FoolsGold* [12] exclude a client's model updates that have outlier cosine similarity in values to other clients' model updates. *FLAIR* [33] and *RobustLR* [27] reduce or penalize the contribution of model updates that show a certain degree of sign dissimilarity, either on a client-wise or element-wise basis.

Excluding model updates that are outliers in certain features: Some existing works believed that the effects of backdoor attacks could be reflected on some features extracted from model updates' values, so they proposed to filter model updates according to certain features. *BayBfed* [19] and *FreqFed* [11] assess the probabilistic distribution and frequency transformation of clients' model updates, and eliminate outlier clients based on these features. *FRL* [25] creates a sparse space of model updates for clients to vote, where the server rejects outlier votings and aggregates the acceptable updates within this space.

Byzantine-robust aggregation: Some existing works propose aggregating only the most trustworthy model updates to tolerate the presence of malicious clients, which we refer to as byzantine-robust aggregation. *Median* and *Trimmed Mean* [42] aggregate reliable model updates element-wise, while *Multi-Krum* [3] and *RFA* [28] select and aggregate reliable model updates client-wise. *FLCert* [6] takes the majority inference results from the reliable models of different client groups to mitigate the influence of malicious clients.

Analyzing clients' model updates can effectively defend against backdoor attacks with static objectives due to the great divergence existing between malicious clients' and benign clients' model updates. However, when a backdoor attack can dynamically change its ob-

jective to effectively eliminate the difference between a client's model updates in malicious state and benign state, defenses based on this strategy may struggle to succeed.

3 Threat Model

Attacker's capability: As shown in Figure 3, we assume that each FL client—even a malicious one—is equipped with trustworthy training software that conducts correct model training on the client's local training data and transmits the model updates to the FL server. Aligning with the security settings in the state-of-the-art defense work [29], we assume that both the client training pipeline and the FL server, as well as the communication between them, faithfully serve FL's main task training and cannot be undetectably manipulated. These properties would be achievable by executing FL training within Trusted Execution Environments (TEEs) [31, 29], for example, by applying cryptographic protections to the updates (e.g., a digital signatures) to enable the FL server to authenticate the updates as coming from the TEEs.

Due to the TEE's protections, malicious clients are not allowed to conduct any model poisoning. The capability of malicious clients in our attack is limited to the manipulation of their local training data that are input to their training pipelines—i.e., a data-poisoning attack. In addition, in line with existing works [22, 44, 10, 14], we do not assume the secrecy of the global model provided by the FL server, as it would typically need to be accessible outside TEEs for use in local inference tasks. As such, in each FL round, clients are granted white-box access to the global model.

Attacker's background knowledge: In our attack, we consider the presence of malicious clients in the FL system. As discussed above, malicious clients can white-box access to the global model in each round. Originating from initially benign clients that have been compro-

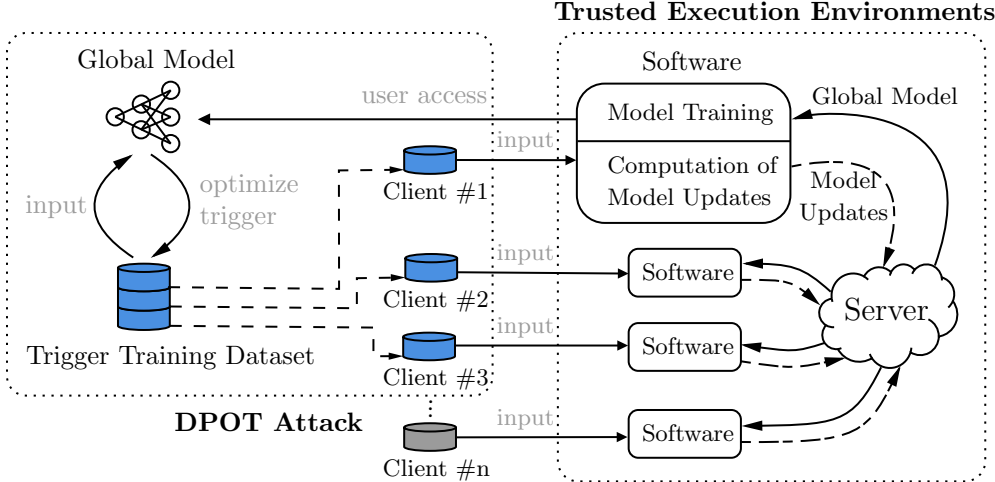


Figure 3: Overview of DPOT attack process on a FL system within Trusted Execution Environments (TEEs). In each global round of FL, DPOT attack comprises three key stages: the construction of a Trigger Training Dataset, Trigger Optimization, and the Data Poisoning to the malicious clients. In this figure, Client #1, #2, and #3 perform as the malicious clients while other clients (e.g. Client #n) are benign clients.

mised, these malicious clients possess some local training data for the FL main task.

Attacker’s goals: The malicious clients aim to accomplish the following goals.

- **Effectiveness.** By convention, *Attack Success Rate* (ASR) is used to assess the effectiveness of a backdoor attack. For classification tasks, ASR is defined as the accuracy of a model in classifying data embedded with a backdoor trigger into the target label associated with this trigger. The DPOT attack aims to cause the global model in each FL round to misclassify data embedded with a backdoor trigger, generated in the previous round, into a target label. Our effectiveness goal is for the global model to achieve an ASR of over 50% in the final round and even maintain an average ASR of over 50% across all rounds.
- **Stealthiness.** The stealthiness goal of a backdoor attack is to maintain the *Main-task Accuracy* (MA) of the global model at a normal level, ensuring the functionality of the global model on its main-task data. Specifically, we require that the compromised global model resulting from our attack has a similar MA (± 2 percentage points) compared to a global model that has not been subjected to any attacks.

4 DPOT Design

4.1 Overview

In each round of FL (e.g., the i -th round), DPOT attack takes place after the malicious clients receive the global model $W_g^{(i)}$ of this round but before they input their local training data to the trustworthy training software.

Given a global model $W_g^{(i)}$ and a pre-defined target label y_t , we optimize the pattern of a backdoor trigger to increase the ASR of $W_g^{(i)}$. By poisoning malicious clients’ local training data using this optimized trigger $\tau^{(i)}$, we expect that the global model of the next round $W_g^{(i+1)}$ will also exhibit a high ASR in classifying data embedded with $\tau^{(i)}$ into its target label y_t .

To achieve this goal, we first construct a trigger training dataset by collecting data from malicious clients. After changing the labels of all data in the trigger training dataset to be the target label y_t , we compute the gradient on each pixel of each image with respect to the loss of $W_g^{(i)}$ in misclassifying each clean image into label y_t . We determine trigger-pixel placements E_t within the pixel location space of an image by selecting tri_{size} number of pixels that demonstrate largest absolute values among the pixel-wise sum of gradients from all images. Next, we optimize each pixel’s value in E_t using gradient descent, obtaining the trigger-pixel values V_t . Finally, we embed the optimized trigger defined by (E_t, V_t) with its target label y_t into malicious clients’ local training data at a certain poison rate.

4.2 Building a Trigger Training Dataset

At the beginning of the DPOT attack, we initially gather all available benign data from the malicious clients’ local training datasets and assign a pre-defined target label y_t to them. We refer to this new dataset, which associates benign data with the target label, as the trigger training dataset D .

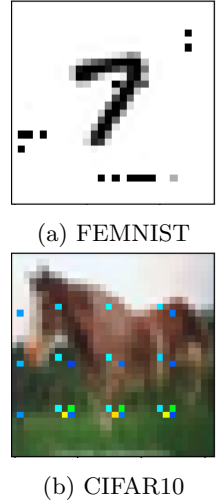


Figure 4: Poisoned data with DPOT triggers.

4.3 Optimizing Backdoor Trigger

Formulating an optimization problem: We use the trigger training dataset to generate a different backdoor trigger for each round’s global model. The optimization process operates independently across the rounds of FL, implying that generating a backdoor trigger for the current round’s global model does not depend on any information from previous rounds. Therefore, in this part, we introduce the trigger optimization algorithms within a single round of FL.

In the image classification context, consider the global model W_g as input and all pixels within an image as the parameter space. Our approach aims to find a subset of parameters that have the most significant impact in producing the malicious output result (i.e., target label), and subsequently optimize the values of the parameters in this subset for the malicious objective (i.e., a high ASR). In the end, the pixels in this subset with their optimized values will serve as a backdoor trigger. This trigger will increase the likelihood that an image containing it will yield the malicious output when employing the same model W_g for inference. The optimization objective to resolve the above problem can be written as formula 1.

$$\min_{\tau} \frac{1}{|D|} \sum_{x \in D} \text{Loss}(W_g(x \odot \tau), y_t), \quad (1)$$

where τ represents the backdoor trigger composed of trigger-pixel placements E_t and trigger-pixel values V_t . The objective is to minimize the difference between the target label y_t and the output results of the global model W_g when taking the backdoored images as input, which can be quantified by a loss function. The symbol \odot represents an operator to embed the backdoor trigger τ into a clean image x , whose definition is further described in (2) of Section 5. To enhance generalization performance of the optimized backdoor trigger, we employ all images in the trigger training dataset D as constraints and try to find a backdoor trigger that takes effect for all of these images.

Solving the optimization problem: To solve the above optimization problem, our approach employs two separate algorithms: one for computing the trigger-pixel placements E_t (see Algorithm 1), and the other for optimizing the trigger-pixel values V_t using E_t as input (see Algorithm 2).

Compute trigger-pixel placements E_t . In Algorithm 1, we select pixel locations that contain the largest absolute gradient values with respect to the backdoor objective (1) as the trigger-pixel placements.

Algorithm 1 takes several inputs, including the global model W_g , the trigger training dataset D , the target

Algorithm 1 Computation for Trigger-pixel Placements

Input: W_g, D, y_t, tri_size

Output: E_t

- 1: $\forall x \in D : y_x \leftarrow W_g(x)$.
 - 2: $\mathcal{L} \leftarrow \frac{1}{|D|} \sum_{x \in D} (y_x - y_t)^2$.
 - 3: $\forall x \in D : \delta_x \leftarrow \frac{\partial \mathcal{L}}{\partial x}$.
 - 4: $\delta \leftarrow abs(\sum_{x \in D} \delta_x)$.
 - 5: $\delta_f \leftarrow$ flatten δ into a one-dimensional array.
 - 6: $S \leftarrow argsort(\delta_f)$. {Store the sorted indices (descending sort)}
 - 7: $E_t \leftarrow S[1 : tri_size]$. {Top tri_size indices are trigger placements}
 - 8: $E_t \leftarrow$ transform from one-dimensional indices to indices for $x \in D$.
 - 9: **return** E_t
-

label y_t , and a parameter tri_size that specifies the trigger size. The trigger size tri_size determines the number of pixel locations we will choose. The output of the Algorithm 1 is the trigger-pixel placement information denoted as E_t .

Starting from line 1 and line 2, we first calculate the loss of the global model W_g in predicting clean images in dataset D as the target label y_t , where we show Mean Square Error (MSE) as an example loss function. Next, we compute the gradient of the loss with respect to each pixel in each image and store the values of gradients in each image x in δ_x (line 3). After summing up δ_x per pixel and take the absolute value of the results, we obtain an absolute gradient value matrix with the same shape as an individual image in dataset D (line 4). To better describe how we sort elements in δ by their values, we first flatten δ into a one-dimensional array δ_f (line 5), and then sort elements in this array in descending order and store the sorted indices in an array S (line 6). The top tri_size number of indices are the trigger-pixel placements of interest, but before returning these indices, we transform them from indices for a one-dimensional array to indices for a matrix of an image’s shape in dataset D (line 7, line 8).

Optimize trigger-pixel values V_t . In Algorithm 2, we optimize the values of the trigger pixels defined in E_t using a learning-based approach.

Algorithm 2 requires the following inputs: the trigger-pixel placements E_t , the global model W_g , the trigger training dataset D , and the target label y_t . Additionally, it uses two training parameters: the number of training iterations n_{iter} and the learning rate γ . The output produced by Algorithm 2 is the trigger-pixel value information denoted as V_t .

The first step of each iteration is making a copy dataset D' of D (line 2) so that the optimized trigger

Algorithm 2 Optimization for Trigger-pixel Values

Input: $E_t, W_g, D, y_t, n_{iter}, \gamma$ **Output:** V_t

```
1: for iteration  $\leftarrow$  1 to  $n_{iter}$  do
2:    $D' \leftarrow D$ .
3:   if iteration = 1 then
4:      $V_t \leftarrow \frac{1}{|D'|} \sum_{x \in D'} x$ .
5:   else if iteration > 1 then
6:      $\forall x \in D' : x[E_t] \leftarrow V_t[E_t]$ .
7:   end if
8:    $\forall x \in D' : y_x \leftarrow W_g(x)$ .
9:    $\mathcal{L} \leftarrow \frac{1}{|D'|} \sum_{x \in D'} (y_x - y_t)^2$ .
10:   $\forall x \in D' : \delta_x \leftarrow \frac{\partial \mathcal{L}}{\partial x}$ .
11:   $\delta \leftarrow \sum_{x \in D'} \delta_x$ .
12:   $V_t[E_t] \leftarrow (V_t - \gamma \cdot \delta)[E_t]$ .
13: end for
14: return  $V_t$ 
```

of each iteration can always be embedded into clean data. In the first iteration, we initialize the trigger-pixel value matrix V_t by taking the mean value of all images in dataset D' along each pixel location (line 4). Then, we calculate the loss of the global model W_g in predicting images from D' as the target label y_t (line 8, 9). Next, we compute the gradients of the loss with respect to each pixel in each image in dataset D' and store the values of gradients in each image x in δ_x (line 10). The gradient matrix δ is obtained by summing up δ_x along each pixel location (line 11) (but not need to take the absolute value as Algorithm 1). After that, we use the gradient descent technique with γ as the learning rate to only update the values of pixels within the trigger-pixel placements E_t (line 12) and assign those new values to the trigger value matrix V_t . For all iterations after the initial one, we consistently replace pixels within the trigger-pixel placements E_t of each image with their corresponding values in the trigger value matrix V_t (line 6). The steps of line 6 and line 12 ensure that the only variables influencing the loss result are the pixels specified by E_t .

4.4 Poisoning Malicious Clients' Training Data

The last step of our attack is to poison malicious clients' local training data using the optimized trigger $\tau = (E_t, V_t)$ and its target label y_t by a certain data poison rate. The data poison rate can be specified on a scale from 0 to 1, while smaller data poison rate induces stealthier model updates, making them more difficult for defenses to detect and filter. In the following, we set the data poison rate to 0.5 for all experiments.

5 Theoretical Analysis

In this section, we delve into the reasons behind DPOT's ability to successfully bypass state-of-the-art defenses, and analyze the improvements of an optimized trigger generated by our algorithms in assisting backdoor attacks, compared to a fixed trigger.

We use a linear regression model to explain the intuition of this work. Consider a regression problem to model the relationship between a data sample and its predicted values. We define $x \in \mathcal{D}^{1 \times n}$, where \mathcal{D} is a convex subset of \mathbb{R} as a data sample, and the vector $\hat{y} \in \mathbb{R}^{1 \times m}$ as its target values. The model $\beta \in \mathbb{R}^{n \times m}$ that makes $x\beta = \hat{y}$ is what we want to solve.

For any given data x , a backdoor attack is aiming to make the model β fit both the benign data point (x, \hat{y}) and the corresponding malicious data point (x_t, y_t) . We use $y_t \in \mathbb{R}^{1 \times m}$ to represent the backdoor target values and specify that $y_t \neq \hat{y}$. $x_t \in \mathcal{D}^{1 \times n}$ is the data x embedded with a trigger τ by the following operation.

$$x_t = x(I_n - E_t) + V_t E_t, \quad (2)$$

where $V_t \in \mathcal{D}^{1 \times n}$ is a vector storing the trigger τ 's value information, and $E_t \in \{0, 1\}^{n \times n}$ is a matrix identifying the trigger τ 's location information. E_t specifies the location and shape of the trigger, defined as $E_t = \text{diag}(d_1, d_2, \dots, d_n)$, $d_i \in \{0, 1\}$, where $\sum_{i=1}^n d_i = k$. Here, k defines the number of entries in the original x that we intend to alter. The abbreviation $\text{diag}(\cdot)$ stands for a diagonal matrix whose diagonal values are specified by its arguments. I_n is an $n \times n$ identity matrix.

Definition 5.1. (Benign Loss and Benign Objective) Let $x \in \mathcal{D}^{1 \times n}$ be a benign data sample, $\hat{y} \in \mathbb{R}^{1 \times m}$ be the predicted value of x , and $\beta \in \mathbb{R}^{n \times m}$ be the prediction model. The loss to evaluate the prediction accuracy of β on the benign regression is

$$L(x, \hat{y}) = \|x\beta - \hat{y}\|_2^2. \quad (3)$$

The optimization objective to solve for β for this benign task is

$$\min_{\beta} L(x, \hat{y}). \quad (4)$$

Definition 5.2. (Backdoor Loss and Backdoor Objective) Let x_t be a backdoored data sample embedded with a trigger $\tau(V_t, E_t, y_t)$. Let $\beta \in \mathbb{R}^{n \times m}$ be the prediction model. The loss to evaluate the prediction accuracy of β on the backdoor regression is

$$L(x_t, y_t) = \|x_t \beta - y_t\|_2^2. \quad (5)$$

The optimization objective to solve for β for the backdoor task that considers both benign data and backdoor data is

$$\min_{\beta} (1 - \alpha)L(x, \hat{y}) + \alpha L(x_t, y_t), 0 \leq \alpha \leq 1. \quad (6)$$

The FL global model learns backdoor information only when it integrates malicious clients’ model updates that were trained for the backdoor objective. Due to the implementation of robust aggregation, backdoor attackers have to ensure their model updates have limited divergence from those trained on benign data to avoid being filtered out by defense techniques. We term this intention as the concealment objective.

To formulate the above problem, we use gradients of optimizing the benign objective (G_{bn}) and gradients of optimizing the backdoor objective (G_{bd}) with respect to a same model β to represent model updates of a benign client and a malicious client respectively. We then use cosine similarity as a metric to evaluate the difference between G_{bn} and G_{bd} , since it is a widely used metric in the state-of-the-art defenses [5, 26, 33, 12] to filter malicious model updates.

G_{bn} and G_{bd} are computed by

$$G_{bn} = \frac{\partial L(x, \hat{y})}{\partial \beta}, \quad (7a)$$

$$G_{bd} = \frac{\partial ((1 - \alpha)L(x, \hat{y}) + \alpha L(x_t, y_t))}{\partial \beta}. \quad (7b)$$

The concealment objective is

$$\max \text{CosSim}(G_{bn}, G_{bd}). \quad (8)$$

The optimization objective used in DPOT attack is

$$\min_{V_t, E_t} \| (x(I_n - E_t) + V_t E_t)\beta - y_t \|_2^2. \quad (9)$$

Proposition 5.1. *Given a model β and a data sample x with its benign predicted value \hat{y} and a backdoor predicted value y_t , the optimization of objective (9) is a guarantee of the optimization of objective (8).*

Proof. See proof in Appendices B.1. \square

Proposition 5.1 offers a theoretical justification for DPOT’s ability to prevent malicious clients’ model updates from being detected by a commonly used metric considered in state-of-the-art defenses. In Proposition B.1 and Proposition 5.2, we demonstrate that an optimized trigger ($\hat{\tau}$) generated by learning the parameters of a given model β is more conducive to achieving the concealment objective compared to a trigger (τ_f) with fixed value, shape, and location.

Proposition 5.2. *For any fixed trigger $\tau_f(V_t, E_t, y_t)$ with specified trigger value V_t , trigger location E_t , and predicted value y_t , there exists a backdoor trigger $\hat{\tau}(\hat{V}_t, \hat{E}_t, y_t)$ that has the same y_t , but optimizes the V_t and E_t with respect to a model β , which can result in a smaller or equal backdoor loss on model β compared to τ_f .*

Proof. See proof in Appendices B.3. \square

6 Experiments

6.1 Experimental Setup

Datasets and global models: We evaluated DPOT on four classification datasets with non-IID data distributions: Fashion MNIST, FEMNIST, CIFAR10, and Tiny ImageNet. Table 1 summarizes their basic information and models we used on each dataset.

Table 1: Dataset description

Dataset	#class	#img	img size	Model	#params
Fashion MNIST	10	70k	28 × 28 grayscale	2 conv 3 fc	~1.5M
FEMNIST	62	33k	28 × 28 grayscale	2 conv 2 fc	~6.6M
CIFAR10	10	60k	32 × 32 color	ResNet18	~11M
Tiny ImageNet	200	100k	64 × 64 color	VGG11	~35M

Comparisons: As DPOT is exclusively a data-poisoning attack, we compared it with existing attacks where all the non-data-poisoning components were removed. To be specific, we only implemented the trigger embedding part introduced in existing attacks, while disregarding any model-poisoning techniques such as objective modification, alterations to training hyperparameters, or scaling up malicious model updates.

We compared DPOT with three existing attacks as described below.

- **Fixed Trigger (FT).** Following recent research on backdoor attacks on FL [2, 39, 5, 1], pixel-pattern triggers are typical backdoors applied in image classification applications. A pixel-pattern trigger is a defined arrangement of pixels with specific values and shape, placed at a particular location within images. We used a global pixel-pattern trigger with fixed features (values, shape, and placement) for all experiments in this attack category.
- **Distributed Fixed Trigger (DFT).** Inheriting the definition of the pixel-pattern trigger, DBA [39] slices a global pixel-pattern trigger into several parts and distributes them among different malicious FL clients for data poisoning. The Attack Success Rate for this attack category is evaluated based on the global pixel-pattern trigger.
- **A3FL Trigger.** A state-of-the-art attack in FL, A3FL [44], proposed adversarially optimizing the trigger’s value using a local model that continuously unlearns the optimized trigger information. The shape and placement of the A3FL trigger stay fixed during optimization. We compare their methods on CIFAR10 dataset as it is the only available configuration in their open-source project.

The visualization of various trigger types are demonstrated in Figures 6, 7, 8, and 10.

Defenses: We evaluated backdoor attacks in FL systems employing different state-of-the-art defense strategies against backdoor attacks. We selected defense baselines based on two criteria: 1) Defenses provided accessible proof-of-concept codes to ensure accurate implementation of their proposed ideas; 2) Defenses either claimed or were proven by existing research to have defense effectiveness against backdoor attacks in FL.

We presented the evaluation results of 10 defense strategies that rely solely on server-side execution in Section 6. Detailed descriptions of these defenses were presented in Appendices C. The evaluation results of defenses requiring client-side execution, Flip [45] and FRL [25], were demonstrated in Appendices E and Appendices F due to space limitations.

Evaluation metrics: We considered three metrics to evaluate the effectiveness and stealthiness of backdoor attacks when confronted with different defense strategies.

Final Attack Success Rate (Final ASR). This metric quantifies the proportion of backdoored test images that were misclassified as the target label by the global model at the end of training. In order to reduce the testing error caused by noise on data or model so as to maintain the fairness of comparison, we tested ASR on the global models of the last five rounds and took their mean value as the Final ASR .

Average Attack Success Rate (Avg ASR). We initiate the attack from the first round of FL training. Since the attack cycle of DPOT spans just a single round, we introduced Avg ASR to assess the average attack effectiveness across all rounds during the FL process. To evaluate ASR for an individual round, we poison test data with the optimized trigger $\tau^{(i)}$ which is generated using the current-round global model $W_g^{(i)}$ and test its ASR on the next-round global model $W_g^{(i+1)}$. We took the average of the ASR of all rounds in the FL process as the Avg ASR . The implication of a high Avg ASR of an attack is that this attack had consistently significant effectiveness during the whole FL process, ensuring a high Final ASR no matter when the FL process ended.

Main-task Accuracy (MA). We evaluate this metric by testing the accuracy of a global model on its clean main-task test dataset. A backdoor attack is seen to be stealthy if its victim model does not show a noticeable reduction in MA compared to the benign model.

FL configurations: The FEMNIST dataset [4] provides each client’s local training data with a naturally non-IID guarantee. For Fashion MNIST, CIFAR10, and Tiny ImageNet datasets, we distributed training data

to FL clients using the same method introduced by FLTrust [5], where we set the non-IID bias to be 0.5.

For all datasets training experiments, we used SGD optimization with CrossEntropy loss. In the experiments on Tiny ImageNet, we set the mini-batch size to 64, while for the other datasets, we set it to 256. Each FL client trained a global model for $n_{epoch} = 5$ local epochs with its local data in one global round.

For training Fashion MNIST and FEMNIST datasets, we used a static local learning rate (lr) of 0.01. For training the larger and more complicated datasets such as CIFAR10 and Tiny ImageNet, we applied the learning rate schedule technique following the instructions in the related machine learning works [16, 34] to boost DNN models’ performance.

Attack configurations: In our algorithm 2 for training a trigger value, we set the number of training iterations to $n_{iter} = 10$, which proved sufficient for obtaining the optimal trigger values. The learning rate γ started from 5 and was halved when the training loss increased compared to the previous iteration.

Table 2 shows the default settings of DPOT attack for experiments. In particular, we consider the following attributes that are critical for attack effectiveness.

Table 2: Default Settings

	Fashion MNIST	FEMNIST	CIFAR10	Tiny ImageNet
Trigger Size	64	25	25	64
Round	300	200	150	100
Number of Clients	100	100	50	50
MCR	0.05			
Local Data PoisonRate	0.5			

Trigger size. We defined trigger size for different datasets according to the following three criteria. First, a trigger of the defined trigger size should not be able to cover important details of any images and lead humans to misidentify the images from their original labels. To show that we follow this criteria, we demonstrated poisoned images from different datasets that are embedded with DPOT triggers, as shown in Figure 4 and 9. Second, on basis of the first criterion, we adjust trigger size to match the image size and the feature size of different datasets. Specifically, if a dataset contains images with high resolution (large image size), then a large trigger size is needed to effectively match it (Tiny ImageNet vs. CIFAR10). If images in a dataset contain large visual elements or patterns, then a large trigger size is needed to effectively match it (Fashion MNIST vs. FEMNIST). Third, we found that when using models with deep model architectures or having large number of pa-

rameters, a small trigger size is sufficient for conducting DPOT attack (CIFAR10 vs. Fashion MNIST).

Round. We determine the number of training rounds for each dataset by measuring the convergence time on an FL pipeline using FedAvg as the aggregation rule. Convergence is considered achieved when the test accuracy on the main task stabilizes within a range of 0.5 percentage points over a period of five consecutive rounds of training.

Number of clients. The number of clients varies across different datasets due to a balance between our available computational resources and the size of the datasets/models. All clients participate in the aggregation for each round of FL training.

MCR. Malicious Client Ratio (MCR) is a parameter defining the proportion of compromised clients compared to the total number of clients in each-round aggregation. We consider 5% as the default MCR (for FL systems having 50 clients, 2 of them are malicious clients), which is smaller than the state-of-the-art attacks [44, 22, 10] that require at least 10% of clients to behave maliciously during aggregation.

Local data poison rate. It indicates the proportion of data manipulated by a backdoor attack relative to the total data available on each malicious client.

Experiment environment and code: We conducted all the experiments on a platform with multiple NVIDIA Quadro RTX 6000 Graphic Cards having 24 GB GPU memory in each chip and an Intel(R) Xeon(R) Gold 6230 CPU @2.10GHz having 384 GB CPU memory. We implemented all the algorithms using the PyTorch framework. We will open-source this project after its publication.

6.2 Experimental Results

6.2.1 Representative Results

In this section, we presented the performance of DPOT attack under 10 defense methods and compared our results with two widely-used data-poisoning attacks.

The effectiveness of an attack is measured using the *ASR* metric, as shown in Figure 5. Results indicate that the DPOT attack consistently achieves a final *ASR* exceeding 50% across all considered defense methods, regardless of the dataset’s characteristics such as image size and number of images. Additionally, the DPOT attack also exhibits a considerable average *ASR* in each attack practice, indicating its malicious effect on each-round global model. The stealthiness of an attack is assessed using the *MA* metric, as indicated in Table 8. We established a baseline *MA* for each defense method on every dataset by measuring the final *MA* achieved in an attack-free FL training session employing the respective defense. Upon comparing the baseline *MA* of

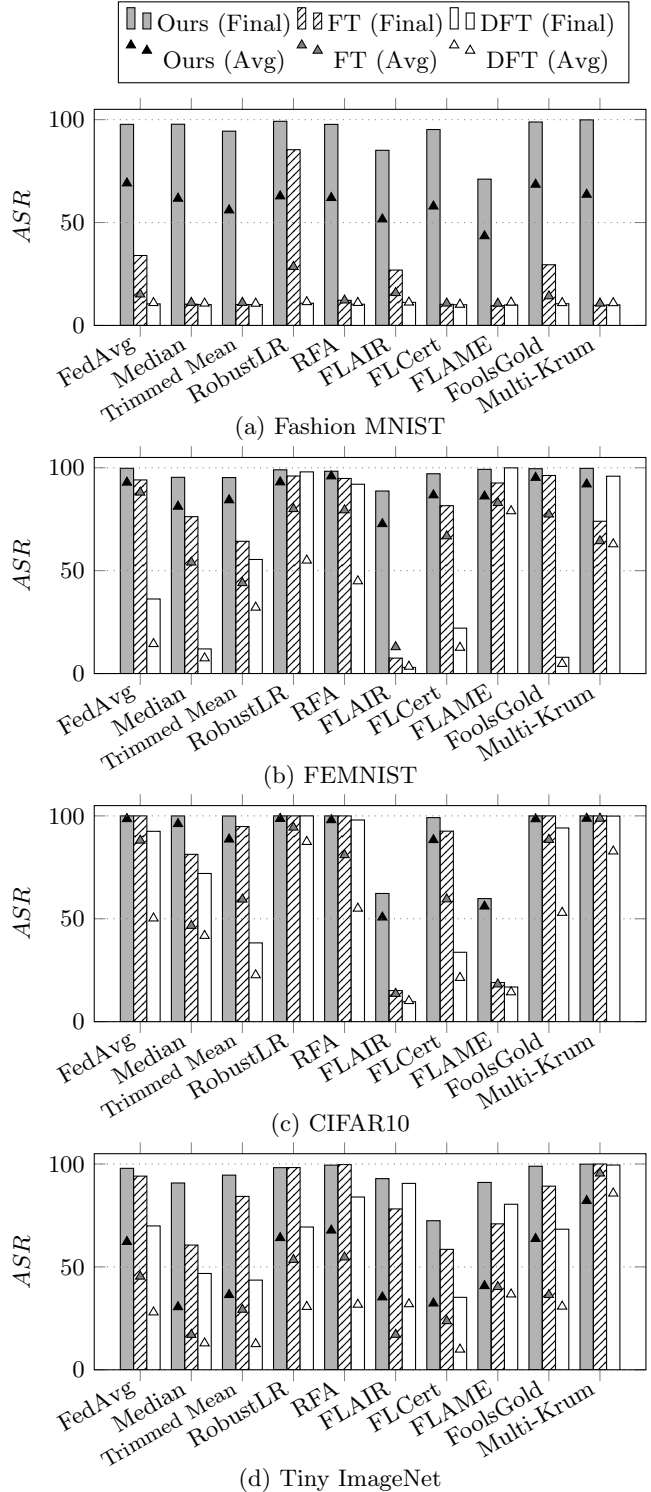


Figure 5: Representative results on four different datasets are provided. The attack settings correspond to the default settings outlined in Table 2.

various defenses to that of FedAvg, we observed that certain defenses, such as Multi-Krum on most of datasets and FLAME on Tiny ImageNet, failed to achieve similar convergence performance as FedAvg under the same

training conditions. Defenses with deficient baseline MA are less likely to be adopted in practice. The results presented in Table 8 indicate that the DPOT attack successfully maintains the MA of victim global models within a ± 2 percentage-point difference range compared to the corresponding baseline MA values.

In comparison to FT and DFT attacks, the DPOT attack demonstrates superior attack effectiveness in compromising existing defenses. As illustrated in Figure 5, the DPOT attack consistently demonstrates a higher Final ASR compared to FT and DFT attacks and also achieves a significantly better Average ASR.

6.2.2 Comparison to A3FL Trigger

	Final ASR		Average ASR		MA	
	Ours	A3FL	Ours	A3FL	Ours	A3FL
FedAvg	100	48.9	98.5	38.1	70.7	70.6
Median	100	32.9	96.1	24.0	69.1	69.1
Trimmed Mean	100	35.0	88.6	23.5	70.4	69.9
RobustLR	100	46.2	98.6	40.7	70.1	71.2
RFA	100	24.7	97.8	23.8	70.7	70.2
FLAIR	62.3	13.2	50.7	12.5	70.6	70.7
FLCert	99.2	39.0	88.3	28.4	70.0	69.9
FLAME	59.8	13.7	56.0	32.1	70.3	70.1
FoolsGold	100	46.9	98.5	38.0	71.0	70.8
Multi-Krum	100	33.4	98.7	29.5	63.0	62.8

Table 3: Comparison results with A3FL attack on CIFAR10.

In this section, we compared the performance of DPOT attack with the A3FL [44] attack. We implemented the A3FL attack by faithfully replicating the attacker’s actions as designed by A3FL, with reference to their open-source project. We evaluated the effectiveness of A3FL attack against 10 defense strategies within our FL configurations and attack settings (refer to Table 2).

The results in Table 3 demonstrate that our attack achieved significantly higher ASR values in both the final and average metrics compared to the A3FL attack. This suggests that the optimized triggers generated using our algorithms are more effective in compromising FL global models through data poisoning compared to those generated using A3FL’s techniques. Additionally, we observed that the ASR results of A3FL were even worse than those of FT and DFT (as shown in Figure 5) in our experiment settings. This implies that dynamically changing the backdoor objective may not enhance the effectiveness of backdoor attacks compared to maintaining a static backdoor objective if it can not align to the benign objective effectively.

6.2.3 Analysis of the DPOT working principles

In this section, we analyzed the attack effectiveness of each component of the DPOT attack’s working principles and report evidence that it effectively conceals malicious clients’ model updates, thereby getting them integrated into the global models through aggregation.

In the i -th round, DPOT generates a trigger $\tau^{(i)}$ by optimizing its shape, placement and values to make the global model of this round $W_g^{(i)}$ achieve a maximum ASR . However, what we were truly interested in is its ASR on the global model after the i -th round aggregation, which is the next-round global model denoted as $W_g^{(i+1)}$. The attack effectiveness of the trigger $\tau^{(i)}$ on the global model $W_g^{(i+1)}$ stems from two factors:

- Trigger Optimization:** Trigger optimization using $W_g^{(i)}$ results in an improvement of the trigger’s ASR on $W_g^{(i+1)}$ due to the small difference between $W_g^{(i+1)}$ and $W_g^{(i)}$.
- Concealment of Model Updates:** Model updates that were trained on data partially poisoned by $\tau^{(i)}$ exhibit small differences from those were trained on data without poisoning. Therefore, they were aggregated into $W_g^{(i+1)}$ and made $W_g^{(i+1)}$ incorporate backdoored model parameters.

In the following, we explain how we designed experiments to study the impact of each factor, and analyzed the experiment results.

Experiment design: To assess the attack effectiveness solely brought by Trigger Optimization, we eliminated any effects produced by data poisoning. Specifically, we set all clients in the FL system to be benign, ensuring that the next-round global model, denoted as $\widetilde{W}_g^{(i+1)}$, aggregated benign model updates only. In the meantime, we still collected data from a certain number of clients and optimized a trigger $\widetilde{\tau}^{(i)}$ for $\widetilde{W}_g^{(i)}$. Then, we tested $\widetilde{W}_g^{(i+1)}$ on a testing dataset in which all images are poisoned with the trigger $\widetilde{\tau}^{(i)}$ to obtain an \widetilde{ASR} . This \widetilde{ASR} evaluates the attack effectiveness achieved by the current-round optimized trigger $\tau^{(i)}$ on the next-round global model $\widetilde{W}_g^{(i+1)}$, which does not contain any model updates learned from backdoor information.

To assess the attack effectiveness brought by Concealment of Model Updates, we introduced malicious clients into the FL system and therefore the global model, denoted as $\ddot{W}_g^{(i+1)}$, was allowed to aggregate model updates submitted by malicious clients. In this system, malicious clients partially poisoned their local training data (aligning with default settings in Table 2) using the trigger $\ddot{\tau}^{(i)}$ that was optimized for $\ddot{W}_g^{(i)}$, and then conducted their local training. We tested the $\ddot{W}_g^{(i+1)}$ on the

		Fashion MNIST		FEMNIST		CIFAR10	
<i>ASR</i> type		Final	Avg	Final	Avg	Final	Avg
FedAvg	\widetilde{ASR}	58.8	45.1	54.0	28.6	55.6	50.9
	\check{ASR}	97.7	69.1	99.7	92.9	100	98.5
Median	\widetilde{ASR}	57.9	38.2	18.0	17.5	56.6	48.7
	\check{ASR}	97.8	61.7	95.4	81.2	100	96.1
Trimmed Mean	\widetilde{ASR}	31.6	29.7	24.2	25.6	55.6	40.9
	\check{ASR}	94.4	56.0	95.2	84.3	100	88.6
RobustLR	\widetilde{ASR}	70.2	47.2	28.8	27.3	60.1	47.3
	\check{ASR}	99.2	62.8	99.3	93.0	100.0	98.6
RFA	\widetilde{ASR}	78.0	46.4	18.9	13.4	57.4	46.1
	\check{ASR}	97.7	62.0	98.3	95.9	100.0	97.8
FLAIR	\widetilde{ASR}	42.2	36.2	23.0	29.6	54.1	45.9
	\check{ASR}	85.3	50.1	88.7	72.7	62.3	50.7
FLCert	\widetilde{ASR}	49.6	39.7	27.7	34.6	48.7	46.7
	\check{ASR}	95.2	57.9	97.1	86.7	99.2	88.3
FLAME	\widetilde{ASR}	38.0	26.2	34.7	35.7	28.1	51.0
	\check{ASR}	71.1	43.4	99.2	86.1	59.8	56.1
Fools-Gold	\widetilde{ASR}	54.2	50.3	57.0	43.7	35.5	35.6
	\check{ASR}	98.9	68.5	99.6	95.2	100	98.5
Multi-Krum	\widetilde{ASR}	60.6	45.4	31.7	28.7	49.7	36.1
	\check{ASR}	99.9	63.6	99.7	92.0	100	98.7

Table 4: *ASR* under different attacking conditions. \widetilde{ASR} assesses the attack effectiveness of “Trigger Optimization” alone, while \check{ASR} assesses the combined effectiveness of both “Trigger Optimization” and “Concealment of Model Updates”.

testing dataset that was also poisoned by $\tilde{\tau}^{(i)}$ to obtain an \check{ASR} . We evaluated the attack effectiveness of Concealment of Model Updates by measuring the increase in *ASR* compared to the previous setting, calculated as $(\check{ASR} - \widetilde{ASR})$. This metric reveals how much the malicious clients’ model updates influenced the global model $\check{W}_g^{(i+1)}$ to achieve a higher *ASR* compared to $\widetilde{W}_g^{(i+1)}$.

Experiment results: Table 4 shows results of \widetilde{ASR} and \check{ASR} over 10 different defense methods. We used same settings as in Table 2 for testing \check{ASR} , and kept the size of trigger training dataset consistent when testing \widetilde{ASR} .

The results of \widetilde{ASR} in Table 4 show that different defense methods resulted in very different \widetilde{ASR} even for the same learning task of a dataset. The reason for the variance of \widetilde{ASR} is the gap between $W_g^{(i)}$ and $\widetilde{W}_g^{(i+1)}$ were different when implementing different defense methods. According to the recent studies [22, 44], if the gap between consecutive rounds of global models in an FL system is smaller, Trigger Optimization will be more effective in its attack.

The results of \check{ASR} in Table 4 show that the presence of malicious clients’ model updates consistently en-

hances *ASR* compared to \widetilde{ASR} across all defense methods on different datasets. We consider this enhancement as an evidence of the statement that the attack effectiveness of DPOT comes from both Trigger Optimization and Concealment of Model Updates, with the latter one playing a critical role in producing a high \check{ASR} .

A general hypothesis made by the state-of-the-art defenses against backdoor attacks in FL is that malicious clients’ model updates have a distinct divergence from benign clients’ model updates. However, as indicated by the results in Table 4, DPOT effectively conceals the model updates from malicious clients amidst those of benign clients, eluding detection and filtering by state-of-the-art defenses. Consequently, defenses formulated based on this broad hypothesis will inherently struggle to defend against DPOT attacks.

6.2.4 Impact of Malicious Client Ratio (MCR)

In this section, we evaluated the impact of different Malicious Client Ratios (MCR) on the attacking performance of DPOT attack. We assumed that the number of malicious clients in the FL system should be kept small ($\leq 30\%$) for practical reasons. We varied the MCR across four different settings (0.05, 0.1, 0.2, and 0.3) while keeping other settings consistent with those in Table 2. We experimented over 10 different defenses on the learning tasks of the CIFAR10 datasets and compare DPOT’s results with FT and DFT.

Tables 5 presents the evaluation results of attack effectiveness. DPOT exhibited a dominant advantage over FT and DFT when the MCR is small (0.05 and 0.1). However, this advantage diminished with increasing MCR, indicating that when a sufficient number of malicious clients present in FL, even FT and DFT can achieve respectable *ASR* against certain defense strategies. In most cases, the *ASR* for all attacks continued to rise as the MCR increased, with the exception of FLAME. Results obtained with FLAME indicate that the number of malicious clients did not significantly impact its defense effectiveness.

Table 9 presents the Main-task Accuracy results for each experiment considered in this section. All MA results for different attacks remain similar to the baseline MA, indicating the correct implementation of each attack.

6.2.5 Impact of Trigger Size

Trigger Size, determining how many pixels in an image we can alter, is an important parameter for DPOT attack. Larger trigger size generally results in a better optimization performance. However, it is essential to strike a balance because an excessively large trigger size will make a trigger obscure important details of images, making the trigger easier to perceive by humans. In this

MCR	Final <i>ASR</i>				Average <i>ASR</i>			
	0.05	0.1	0.2	0.3	0.05	0.1	0.2	0.3
	Ours FT DFT	Ours FT DFT	Ours FT DFT	Ours FT DFT	Ours FT DFT	Ours FT DFT	Ours FT DFT	Ours FT DFT
FedAvg	100 100 93	100 100 100	100 100 100	100 100 100	99 88 50	99 96 88	99 99 92	99 100 97
Median	100 81 72	100 100 97	100 100 100	100 100 100	96 47 42	97 79 63	99 97 82	99 98 93
Trimmed Mean	100 95 38	100 100 99	100 100 100	100 100 100	89 59 23	98 82 69	99 94 85	99 99 92
RobustLR	100 100 100	100 100 100	100 100 100	100 100 100	99 94 87	99 98 94	99 99 98	99 99 99
RFA	100 100 98	100 100 100	100 100 100	100 100 100	98 81 55	99 95 90	99 99 97	99 99 98
FLAIR	62 15 10	58 25 9	67 27 22	82 33 40	51 14 10	64 24 9	68 24 16	84 42 30
FLCert	99 93 34	100 100 95	100 100 100	100 100 100	88 60 21	98 87 60	98 94 83	99 99 91
FLAME	60 19 17	52 18 51	50 16 16	55 19 16	56 18 14	66 19 34	53 19 16	70 23 43
FoolsGold	100 100 94	100 100 100	100 100 100	100 100 100	98 88 53	99 97 87	99 99 95	99 99 98
Multi-Krum	100 100 100	100 100 100	100 100 100	100 100 100	99 99 83	99 100 98	98 100 99	99 100 100

Table 5: The effects of malicious client ratio on the effectiveness of different attacks (CIFAR10).

Trigger Size	Final <i>ASR</i>				Average <i>ASR</i>			
	9	25	49	100	9	25	49	100
	Ours FT DFT	Ours FT DFT	Ours FT DFT	Ours FT DFT	Ours FT DFT	Ours FT DFT	Ours FT DFT	Ours FT DFT
FedAvg	100 94 49	100 100 93	100 100 91	100 100 77	95 60 28	99 88 50	99 90 59	99 93 52
Median	97 23 12	100 81 72	100 95 25	100 99 46	66 21 12	96 47 42	98 66 17	99 82 29
Trimmed Mean	98 51 14	100 95 38	100 99 43	100 100 74	71 29 13	89 59 23	99 74 27	99 79 44
RobustLR	100 100 100	100 100 100	100 100 98	100 100 99	95 91 69	99 94 87	99 94 77	99 95 82
RFA	100 100 99	100 100 98	100 100 100	100 100 98	93 79 56	98 81 55	99 81 71	99 90 73
FLAIR	27 14 14	62 15 10	89 22 15	99 24 14	24 14 13	51 14 10	84 22 15	98 16 13
FLCert	99 38 14	99 93 34	100 88 51	100 100 49	78 26 13	88 60 21	99 59 23	99 78 33
FLAME	21 18 12	60 19 17	100 12 11	100 33 31	35 17 12	56 18 14	84 17 11	90 31 24
FoolsGold	100 100 43	100 100 94	100 100 98	100 100 81	93 72 23	98 88 53	99 94 69	99 94 55
Multi-Krum	100 100 15	100 100 100	99 100 100	100 100 100	99 99 11	99 99 83	99 99 95	99 99 97

Table 6: The effects of trigger size on the effectiveness of different attacks (CIFAR10).

section, we assessed the impact of different trigger sizes on the performance of different attacks. We explored trigger sizes across four different settings (9, 25, 49, and 100) while maintaining other settings in accordance with those outlined in Table 2.

Tables 6 shows that DPOT maintained a significant advantage in *ASR* over FT and DFT across various trigger sizes, ranging from small to large. According to the results, we found that FT and DFT did not benefit from larger trigger sizes in achieving higher *ASR* when encountering with robust aggregations that have advanced defense effectiveness, such as FLAIR and FLAME. A possible explanation on that is when malicious model updates were trained on data poisoned with larger FT or DFT triggers, they exhibited greater divergence from benign model updates, making them more susceptible to detection and filtering by defense mechanisms. In contrast, DPOT demonstrated a continuous improvement in *ASR* as the trigger size increased.

Table 10 presents the Main-task Accuracy results for each experiment considered in this section. Results in it indicate all backdoor attacks achieved their stealthiness goals during attacking.

7 Conclusion and Future Work

In this work, we proposed DPOT, a novel backdoor attack method in federated learning (FL). DPOT dy-

namically adjusts the backdoor objective to conceal malicious clients’ model updates among benign ones, enabling global models to aggregate them even when protected by state-of-the-art defenses. DPOT attack is easy to implement, relying solely on data poisoning, yet it poses a significant threat to existing defense methods.

Future work based on this paper includes extending the research to other learning tasks beyond image classification, such as text generation. Additionally, the time and computational costs of implementing our attack were not discussed, as we assumed attackers could use more powerful resources; thus, optimizing these aspects and developing timing-based defenses will be explored later. Lastly, designing defenses against backdoor attacks like DPOT will need to account for scenarios where a malicious client’s model is indistinguishable from its non-attacked model. It is also crucial to ensure that defenses adhere to FL’s privacy-preserving principles, in line with the primitive version that attracted users to FL.

References

- [1] Eugene Bagdasaryan, Andreas Veit, Yiqing Hua, Deborah Estrin, and Vitaly Shmatikov. How to backdoor federated learning. In *International Conference on Artificial Intelligence and Statistics*, pages 2938–2948. PMLR, 2020.

- [2] Gilad Baruch, Moran Baruch, and Yoav Goldberg. A little is enough: Circumventing defenses for distributed learning. *Advances in Neural Information Processing Systems*, 32, 2019.
- [3] Peva Blanchard, El Mahdi El Mhamdi, Rachid Guerraoui, and Julien Stainer. Machine learning with adversaries: Byzantine tolerant gradient descent. *Advances in neural information processing systems*, 30, 2017.
- [4] Sebastian Caldas, Sai Meher Karthik Duddu, Peter Wu, Tian Li, Jakub Konečný, H Brendan McMahan, Virginia Smith, and Ameet Talwalkar. Leaf: A benchmark for federated settings. *arXiv preprint arXiv:1812.01097*, 2018.
- [5] Xiaoyu Cao, Minghong Fang, Jia Liu, and Neil Zhenqiang Gong. Fltrust: Byzantine-robust federated learning via trust bootstrapping. *arXiv preprint arXiv:2012.13995*, 2020.
- [6] Xiaoyu Cao, Zaixi Zhang, Jinyuan Jia, and Neil Zhenqiang Gong. Flcert: Provably secure federated learning against poisoning attacks. *IEEE Transactions on Information Forensics and Security*, 17:3691–3705, 2022.
- [7] Xinyun Chen, Chang Liu, Bo Li, Kimberly Lu, and Dawn Song. Targeted backdoor attacks on deep learning systems using data poisoning. *arXiv preprint arXiv:1712.05526*, 2017.
- [8] Minghong Fang, Xiaoyu Cao, Jinyuan Jia, and Neil Gong. Local model poisoning attacks to {Byzantine-Robust} federated learning. In *29th USENIX security symposium (USENIX Security 20)*, pages 1605–1622, 2020.
- [9] Minghong Fang, Zifan Zhang, Prashant Khanduri, Songtao Lu, Yuchen Liu, Neil Gong, et al. Byzantine-robust decentralized federated learning. *arXiv preprint arXiv:2406.10416*, 2024.
- [10] Pei Fang and Jinghui Chen. On the vulnerability of backdoor defenses for federated learning. In *Proceedings of the AAAI Conference on Artificial Intelligence*, volume 37, pages 11800–11808, 2023.
- [11] Hossein Fereidooni, Alessandro Pegoraro, Phillip Rieger, Alexandra Dmitrienko, and Ahmad-Reza Sadeghi. Freqfed: A frequency analysis-based approach for mitigating poisoning attacks in federated learning. *arXiv preprint arXiv:2312.04432*, 2023.
- [12] Clement Fung, Chris J. M. Yoon, and Ivan Beschastnikh. The limitations of federated learning in sybil settings. In *23rd International Symposium on Research in Attacks, Intrusions and Defenses (RAID 2020)*, pages 301–316, San Sebastian, October 2020. USENIX Association.
- [13] Clement Fung, Chris JM Yoon, and Ivan Beschastnikh. Mitigating sybils in federated learning poisoning. *arXiv preprint arXiv:1808.04866*, 2018.
- [14] Xueluan Gong, Yanjiao Chen, Huayang Huang, Yuqing Liao, Shuai Wang, and Qian Wang. Coordinated backdoor attacks against federated learning with model-dependent triggers. *IEEE network*, 36(1):84–90, 2022.
- [15] Tianyu Gu, Kang Liu, Brendan Dolan-Gavitt, and Siddharth Garg. Badnets: Evaluating backdoor-attacks on deep neural networks. *IEEE Access*, 7:47230–47244, 2019.
- [16] Kaiming He, Xiangyu Zhang, Shaoqing Ren, and Jian Sun. Deep residual learning for image recognition. In *Proceedings of the IEEE conference on computer vision and pattern recognition*, pages 770–778, 2016.
- [17] Ehsanul Kabir, Zeyu Song, Md Rafi Ur Rashid, and Shagufta Mehnaz. Flshield: A validation based federated learning framework to defend against poisoning attacks. *arXiv preprint arXiv:2308.05832*, 2023.
- [18] Soheil Kolouri, Aniruddha Saha, Hamed Pirsiavash, and Heiko Hoffmann. Universal litmus patterns: Revealing backdoor attacks in cnns. In *Proceedings of the IEEE/CVF Conference on Computer Vision and Pattern Recognition*, pages 301–310, 2020.
- [19] K. Kumari, P. Rieger, H. Fereidooni, M. Jadliwala, and A. Sadeghi. Baybfd: Bayesian backdoor defense for federated learning. In *2023 IEEE Symposium on Security and Privacy (SP)*, 2023.
- [20] Junyu Lin, Lei Xu, Yingqi Liu, and Xiangyu Zhang. Composite backdoor attack for deep neural network by mixing existing benign features. In *Proceedings of the 2020 ACM SIGSAC Conference on Computer and Communications Security*, pages 113–131, 2020.
- [21] Yingqi Liu, Shiqing Ma, Yousra Aafer, Wen-Chuan Lee, Juan Zhai, Weihang Wang, and Xiangyu Zhang. Trojaning attack on neural networks. In *25th Annual Network And Distributed System Security Symposium (NDSS 2018)*. Internet Soc, 2018.

- [22] Xiaoting Lyu, Yufei Han, Wei Wang, Jingkai Liu, Bin Wang, Jiqiang Liu, and Xiangliang Zhang. Poisoning with cerberus: Stealthy and colluded backdoor attack against federated learning. *Proceedings of the AAAI Conference on Artificial Intelligence*, 37:9020–9028, Jun. 2023.
- [23] Brendan McMahan, Eider Moore, Daniel Ramage, Seth Hampson, and Blaise Agüera y Arcas. Communication-efficient learning of deep networks from decentralized data. In *Artificial intelligence and statistics*, pages 1273–1282. PMLR, 2017.
- [24] Xiaoxing Mo, Yechao Zhang, Leo Yu Zhang, Wei Luo, Nan Sun, Shengshan Hu, Shang Gao, and Yang Xiang. Robust backdoor detection for deep learning via topological evolution dynamics. In *2024 IEEE Symposium on Security and Privacy (SP)*, pages 171–171. IEEE Computer Society, 2024.
- [25] Hamid Mozaffari, Virat Shejwalkar, and Amir Houmansadr. Every vote counts: {Ranking-Based} training of federated learning to resist poisoning attacks. In *32nd USENIX Security Symposium (USENIX Security 23)*, pages 1721–1738, 2023.
- [26] Thien Duc Nguyen, Phillip Rieger, Roberta De Viti, Huili Chen, Björn B Brandenburg, Hossein Yalame, Helen Möllering, Hossein Fereidooni, Samuel Marchal, Markus Miettinen, et al. {FLAME}: Taming backdoors in federated learning. In *31st USENIX Security Symposium (USENIX Security 22)*, pages 1415–1432, 2022.
- [27] Mustafa Safa Ozdayi, Murat Kantarcioglu, and Yulia R Gel. Defending against backdoors in federated learning with robust learning rate. In *Proceedings of the AAAI Conference on Artificial Intelligence*, 2021.
- [28] Krishna Pillutla, Sham M. Kakade, and Zaid Harchaoui. Robust aggregation for federated learning. *IEEE Transactions on Signal Processing*, 70:1142–1154, 2022.
- [29] Phillip Rieger, Torsten Krauß, Markus Miettinen, Alexandra Dmitrienko, and Ahmad-Reza Sadeghi. Crowdguard: Federated backdoor detection in federated learning. *arXiv preprint arXiv:2210.07714*, 2022.
- [30] Chamara Sandeepa, Bartłomiej Siniarski, Shen Wang, and Madhusanka Liyanage. Sherpa: Explainable robust algorithms for privacy-preserved federated learning in future networks to defend against data poisoning attacks. In *2024 IEEE Symposium on Security and Privacy (SP)*, pages 204–204. IEEE Computer Society, 2024.
- [31] Moritz Schneider, Ramya Jayaram Masti, Shweta Shinde, Srdjan Capkun, and Ronald Perez. SoK: Hardware-supported trusted execution environments. *arXiv preprint arXiv:2205.12742*, 2022.
- [32] Ali Shafahi, W Ronny Huang, Mahyar Najibi, Octavian Suci, Christoph Studer, Tudor Dumitras, and Tom Goldstein. Poison frogs! targeted clean-label poisoning attacks on neural networks. *Advances in neural information processing systems*, 31, 2018.
- [33] Atul Sharma, Wei Chen, Joshua Zhao, Qiang Qiu, Saurabh Bagchi, and Somali Chatterji. Flair: Defense against model poisoning attack in federated learning. In *ASIA CCS '23*. Association for Computing Machinery, 2023.
- [34] Karen Simonyan and Andrew Zisserman. Very deep convolutional networks for large-scale image recognition. *arXiv preprint arXiv:1409.1556*, 2014.
- [35] Ziteng Sun, Peter Kairouz, Ananda Theertha Suresh, and H Brendan McMahan. Can you really backdoor federated learning? *arXiv preprint arXiv:1911.07963*, 2019.
- [36] Bolun Wang, Yuanshun Yao, Shawn Shan, Huiying Li, Bimal Viswanath, Haitao Zheng, and Ben Y Zhao. Neural cleanse: Identifying and mitigating backdoor attacks in neural networks. In *2019 IEEE Symposium on Security and Privacy (SP)*, pages 707–723. IEEE, 2019.
- [37] Hongyi Wang, Kartik Sreenivasan, Shashank Rajput, Harit Vishwakarma, Saurabh Agarwal, Jy-yong Sohn, Kangwook Lee, and Dimitris Papailiopoulos. Attack of the tails: Yes, you really can backdoor federated learning. In *Proceedings of the 34th International Conference on Neural Information Processing Systems*, NIPS'20, 2020.
- [38] Kang Wei, Jun Li, Chuan Ma, Ming Ding, Sha Wei, Fan Wu, Guihai Chen, and Thilina Ranbaduge. Vertical federated learning: Challenges, methodologies and experiments. *arXiv preprint arXiv:2202.04309*, 2022.
- [39] Chulin Xie, Keli Huang, Pin-Yu Chen, and Bo Li. Dba: Distributed backdoor attacks against federated learning. In *International Conference on Learning Representations*, 2020.

- [40] Kan Xie, Zhe Zhang, Bo Li, Jiawen Kang, Dusit Niyato, Shengli Xie, and Yi Wu. Efficient federated learning with spike neural networks for traffic sign recognition. *IEEE Transactions on Vehicular Technology*, 71(9):9980–9992, 2022.
- [41] Yuanshun Yao, Huiying Li, Haitao Zheng, and Ben Y Zhao. Latent backdoor attacks on deep neural networks. In *Proceedings of the 2019 ACM SIGSAC conference on computer and communications security*, pages 2041–2055, 2019.
- [42] Dong Yin, Yudong Chen, Ramchandran Kannan, and Peter Bartlett. Byzantine-robust distributed learning: Towards optimal statistical rates. In *International Conference on Machine Learning*, pages 5650–5659. PMLR, 2018.
- [43] XIE Yueqi, Minghong Fang, and Neil Zhenqiang Gong. Fedredefense: Defending against model poisoning attacks for federated learning using model update reconstruction error. In *Forty-first International Conference on Machine Learning*, 2024.
- [44] Hangfan Zhang, Jinyuan Jia, Jinghui Chen, Lu Lin, and Dinghao Wu. A3fl: Adversarially adaptive backdoor attacks to federated learning. *Advances in Neural Information Processing Systems*, 36, 2024.
- [45] Kaiyuan Zhang, Guanhong Tao, Qiuling Xu, Siyuan Cheng, Shengwei An, Yingqi Liu, Shiwei Feng, Guangyu Shen, Pin-Yu Chen, Shiqing Ma, et al. Flip: A provable defense framework for backdoor mitigation in federated learning. *arXiv preprint arXiv:2210.12873*, 2022.
- [46] Zhengming Zhang, Ashwinee Panda, Linyue Song, Yaoqing Yang, Michael Mahoney, Prateek Mittal, Ramchandran Kannan, and Joseph Gonzalez. Neurotoxin: Durable backdoors in federated learning. In *International Conference on Machine Learning*, pages 26429–26446. PMLR, 2022.

Appendices

A Additional Related Works

A.1 Clean-label attacks

Clean-label attacks [32] involve manipulating input data with subtle perturbations while keeping labels unchanged. Although this assumption aligns with scenarios like Vertical Federated Learning [38] (VFL), where participants possess vertically partitioned data with labels owned by only one participant, our study does not consider VFL as our attack scenario. Furthermore, we focus on examining the effects of different backdoor triggers on hiding malicious model updates rather than their imperceptible characteristics. Therefore, discussions of clean-label attacks are beyond the scope of our work.

A.2 Defenses with different privacy-preserving properties

Recent defense works have introduced several unconventional FL pipelines aimed at enhancing the security of FL against various types of attacks. These novel architectures provide different levels of privacy protection and often require additional techniques (e.g., Secured Multi-party Computation) to ensure privacy for FL clients. In light of these privacy considerations, we have chosen to focus our analysis on the conventional FL structure that was originally proposed in the concept of Federated Learning [23]. Although defenses built on newly proposed FL structures fall outside the scope of our main comparison, we offer a discussion of these related works in this section.

Clients’ private data were shared to the server: Some approaches allow the server to have access to a small portion of main-task data shared by clients. To mitigate backdoor attacks, server-side defense strategies use this data to either independently train a model and use its updates as a reference for each round of aggregation (e.g., FLTrust [5]), or to validate clients’ model updates and eliminate those with abnormal outputs (e.g., SSDT [24], SHERPA [30]). However, both of these methods still rely on analyzing clients’ model updates, making them vulnerable to backdoor attacks with dynamic objectives that conceal malicious updates. FedREdefense [43] detects and filters out artificial model updates by reconstructing distilled data shared by clients, but this approach is not effective against backdoor attacks where malicious clients genuinely train their models on poisoned local data rather than fabricating artificial updates.

Clients’ model updates were shared to each other: Some approaches propose allowing clients to

share their model updates with one another, rather than just with the server. CrowdGuard [29] and FLShield [17] suggest that a subset of clients validate other clients’ model updates using their own data, assuming that malicious clients’ updates would produce abnormal outputs on benign data. However, this hypothesis fails when malicious clients’ updates are indistinguishable from non-backdoored updates, a state that can be achieved through backdoor attack with optimized triggers. Fang et al. [9] proposed a decentralized FL framework without a central server, where clients exchange model updates and apply Byzantine-robust aggregation using their own updates as a reference. Like other defenses that rely on analyzing clients’ model updates, this approach is also vulnerable to backdoor attacks with optimized triggers.

B Proofs

B.1 Proof of Proposition 5.1

Proof. The gradient of benign loss (3) with respect to β is

$$g_{bn} = \frac{\partial L(x, \hat{y})}{\partial \beta} = 2x^T(x\beta - \hat{y}).$$

The gradient of backdoor loss (5) with respect to β is

$$g_{bd} = \frac{\partial L(x_t, y_t)}{\partial \beta} = 2x_t^T(x_t\beta - y_t)$$

Gradients G_{bn} and G_{bd} defined by (7a) and (7b) can be written as

$$\begin{aligned} G_{bn} &= g_{bn} \cdot \\ G_{bd} &= (1 - \alpha)g_{bn} + \alpha g_{bd}. \end{aligned}$$

The cosine similarity between G_{bn} and G_{bd} is

$$\begin{aligned} \text{CosSim}(G_{bn}, G_{bd}) &= \frac{g_{bn} \cdot ((1 - \alpha)g_{bn} + \alpha g_{bd})}{|g_{bn}| \cdot |(1 - \alpha)g_{bn} + \alpha g_{bd}|} \\ &= \frac{g_{bn} \cdot (g_{bn} + \frac{\alpha}{1 - \alpha}g_{bd})}{|g_{bn}| \cdot |g_{bn} + \frac{\alpha}{1 - \alpha}g_{bd}|} \end{aligned}$$

One sufficiency to maximize $\text{CosSim}(G_{bn}, G_{bd})$ is to minimize the distance between g_{bn} and $g_{bn} + \frac{\alpha}{1 - \alpha}g_{bd}$, which is

$$\begin{aligned} \Delta d &= |g_{bn} - (g_{bn} + \frac{\alpha}{1 - \alpha}g_{bd})| \\ &= \frac{\alpha}{1 - \alpha} |g_{bd}|. \end{aligned}$$

Since α is a constant, minimizing Δd is equivalent to minimizing $|g_{bd}|$, which is bounded by

$$0 \leq |g_{bd}| = |2x_t^T(x_t\beta - y_t)| \leq 2 |e^T| \cdot |x_t\beta - y_t|,$$

where $e^T \in \mathbb{R}^{1 \times n}$ consists of the largest edge of the domain of x_t , e.g. $\mathbf{1}^T$ if considering normalization.

Thus, the optimization objective is to decrease $|g_{bd}|$ by minimizing its upper bound.

$$\min |x_t\beta - y_t|,$$

which can be achieved by

$$\min_{V_t, E_t} \|(x(I_n - E_t) + V_tE_t)\beta - y_t\|_2^2.$$

□

B.2 Proposition B.1

Proposition B.1. *For any fixed trigger $\tau_f(V_t, E_t, y_t)$ with specified trigger value V_t , trigger location E_t , and predicted value y_t , there exists an optimal backdoor trigger $\hat{\tau}(\hat{V}_t, E_t, y_t)$ that has the same E_t and y_t but optimizes its V_t with respect to a model β , which can result in a smaller or equal backdoor loss on model β compared to τ_f .*

Proof. With a specified location E_t and predicted value y_t , the optimization objective for minimizing backdoor loss is

$$f = \min_{V_t} \|(x(I_n - E_t) + V_tE_t)\beta - y_t\|_2^2$$

Since $V_t \in \mathcal{D}^{1 \times n}$ where \mathcal{D} is a convex domain and $\frac{\partial^2 f}{\partial V_t^2} \succeq 0$ for any $V_t \in \mathcal{D}^{1 \times n}$, $f: \mathcal{D}^{1 \times n} \rightarrow \mathbb{R}$ is a convex function. Thus, there exists an optimal value \hat{V}_t for the objective function f in the domain $\mathcal{D}^{1 \times n}$. □

B.3 Proof of Proposition 5.2

Proof. Assume the value of data x before embedding a trigger is $[x_1, x_2, \dots, x_n]$. If an entry location in x is able to reduce the backdoor loss of β by optimizing its entry value more effectively than any individual entry location within E_t , we incorporate this location into \hat{E}_t . After constructing a \hat{E}_t , we optimize value of entries within \hat{E}_t to obtain the optimized trigger $\hat{\tau}$. We are going to prove that constructing the trigger location \hat{E}_t in this way results in the optimized trigger $\hat{\tau}$ always outperforming the fixed trigger τ_f in terms of backdoor loss.

We use k to represent the number of trigger entries that have been embedded into x . Assume the trigger value V_t is composed of $[v_1, v_2, \dots, v_n]$.

When $k = 0$, the backdoor loss is

$$L(x, y_t)_{k=0} = \|x\beta - y_t\|_2^2.$$

When $k = 1$, we calculate a location of interest i by taking the largest absolute gradient of the $L(x, y_t)_{k=0}$ with respect to all entry locations in x ,

$$i = \arg \max | \frac{\partial L(x, y_t)_{k=0}}{\partial x_i} |.$$

If the entry location i is inside of E_t , according to Proposition B.1, there exists an optimal entry value \hat{v}_i resulting in a smaller or equal backdoor loss compared to v_i . In this case, we save i as one of entry location in \hat{E}_t .

If the entry location i is outside of E_t , we have the following observation:

For any entry location j inside of E_t , we already know

$$| \frac{\partial L(x, y_t)_{k=0}}{\partial x_i} | \geq | \frac{\partial L(x, y_t)_{k=0}}{\partial x_j} |.$$

We use Gradient Descent optimization algorithm to decrease loss by updating the entry value of the selected location with a constant step size Δv . When the selected location is i , the updated loss $L(x^{\{i\}}, y_t)_{k=1}$ will be

$$L(x^{\{i\}}, y_t)_{k=1} = L(x, y_t)_{k=0} - \frac{\partial L(x, y_t)_{k=0}}{\partial x_i} \Delta v,$$

and when the selected location is j , it is

$$L(x^{\{j\}}, y_t)_{k=1} = L(x, y_t)_{k=0} - \frac{\partial L(x, y_t)_{k=0}}{\partial x_j} \Delta v.$$

It can be found that

$$L(x^{\{i\}}, y_t)_{k=1} \leq L(x^{\{j\}}, y_t)_{k=1}.$$

Therefore, i is a better entry location in reducing backdoor loss compared to j when we constrain the updating step size Δv being static. After repeating the optimization step iteratively, if we finally find the optimal entry value \hat{v}_i resulting in a smaller backdoor loss compared to \hat{v}_j , then it must also outperform the fixed value v_j in V_t according to Proposition B.1. If so, we save i as one of entry location in \hat{E}_t . Otherwise, we save j as one of location in \hat{E}_t .

By recursively operating the procedures across $k = 2, 3, \dots$, we will finally construct a \hat{E}_t in which every entry location is proved to contribute a better attack performance than entry locations defined in E_t . □

C Descriptions of Defenses

We implement our attack on FL systems integrated with 9 different defense strategies and provide a brief introduction for each of them:

FedAvg [23], a basic aggregation rule in FL, computes global model updates by averaging all clients' model updates. Despite its effectiveness on the main task, it is not robust enough to defend against backdoor attacks in the FL system.

Median [42], a simple but robust alternative to FedAvg, constructs the global model updates by taking the median of the values of model updates across all clients

Trimmed Mean [42], in our implementation, excludes the 40% largest and 40% smallest values of each parameter among all clients’ model updates and takes the mean of the remaining 20% as the global model updates.

Multi-Krum [3] identifies an honest client whose model updates have the smallest Euclidean distance to all other clients’ model updates and takes this honest client’s model updates as the global model updates. Despite its robustness to prevent the FL system from being compromised by a minor number of adversaries, Multi-Krum is not able to ensure the convergence performance of the FL system on its main task when the data distribution of clients is highly non-IID.

RobustLR [27] adjusts the aggregation server’s learning rate, per dimension and per round, based on the sign information of clients’ updates.

RFA [28] computes a geometric median of clients’ model updates and assigns weight factors to clients depending on their distance from the geometric median. Subsequently, it computes the weighted average of all clients’ model updates to generate the global model updates.

FLAIR [33] assigns different weight factors to clients according to the similarity of the coefficient signs between client model updates and global model updates of the previous round, and then takes the weighted average of all clients’ model updates to form the global model updates. FLAIR requires the knowledge of exact number of malicious clients existing in the FL system.

FLCert [6] randomly clusters clients, calculates the median of model updates within each cluster, incorporates them into the previous round’s global model, and derives the majority inference outcome from these cluster-updated global models as the final inference result for the entire FL system. In our implementation, we cluster clients into 5 groups, use FLCert inference outcome for testing the Attack Success Rate, and employ Median as the aggregation rule for updating the global model in each round.

FLAME [26] first clusters clients’ model updates according to their cosine similarity to each other, and then aggregates the clipped model updates within the largest cluster as the global model updates.

FoolsGold [13] reduces aggregation weights of a set of clients whose model updates constantly exhibit high cosine similarity to each other.

D Visualization of Triggers

D.1 Different types of trigger on images

We displayed different types of triggers on images from the Tiny ImageNet dataset in Figures 8, 6, and 7. The

Figure 6: FT trigger on Tiny ImageNet data. Training Data 6a and 6b are from different malicious clients. Test Data 6c is used to test ASR.

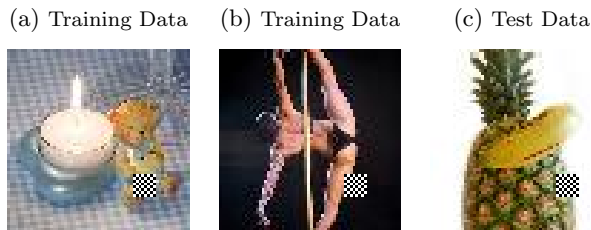


Figure 7: DFT trigger on Tiny ImageNet data. Training Data 7a and 7b are from different malicious clients. Test Data 7c is used to test ASR.

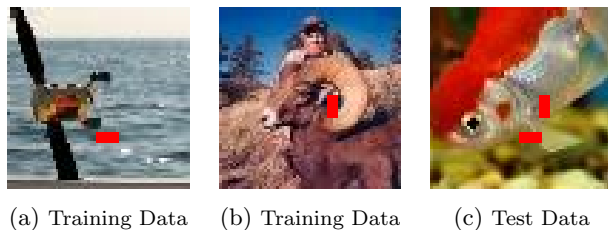
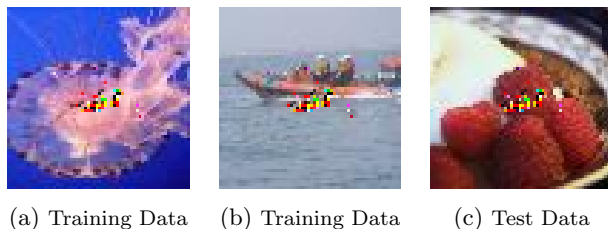


Figure 8: DPOT trigger on Tiny ImageNet data. Training Data 8a and 8b are from different malicious clients. Test Data 8c is used to test ASR.



pattern of the FT trigger remains consistent across all datasets. The DFT triggers shown in Figure 7 are the same as those used for images from the CIFAR10 dataset, while for the Fashion MNIST and FEMNIST datasets, DFT triggers appear in black.

D.2 DPOT triggers on images from different datasets.

We displayed DPOT triggers generated for images from different dataset in Figure 9. Our triggers are in a small size that could not obscure important details of any images.

D.3 A3FL trigger on images of CIFAR10

In Figure 10, we showed triggers generated by A3FL’s methods on images from CIFAR10.

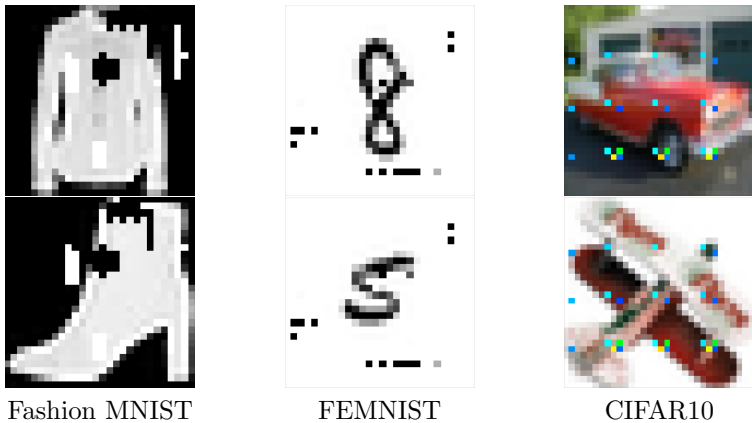


Figure 9: DPOT triggers on images from different datasets.

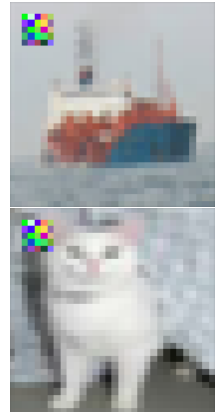


Figure 10: A3FL trigger on images from CIFAR10.

D.4 Trigger evolution during training

In Figure 13 and Figure 14, we demonstrated how DPOT trigger changes during the FL training.

In Figure 13, we showed one screenshot of the trigger on a blank background in the same size of the cifar10’s figure for every ten global rounds. These trigger screenshots were collected during a DPOT attacking experiment that trains ResNet18 as the global model on the CIFAR-10 dataset, with Trimmed Mean used as the aggregation rule. Figure 11 displays the Main-task Accuracy and Attack Success Rate of the global model over 150 global rounds in this experiment.

Similarly, in Figure 14 we showed one screenshot of the trigger on a blank background in the same size of the Tiny ImageNet’s figure for every ten global rounds. These trigger screenshots were collected during a DPOT attacking experiment that trains VGG11 as the global model on the Tiny ImageNet dataset, with Trimmed Mean used as the aggregation rule. Figure 12 displays the Main-task Accuracy and Attack Success Rate of the global model over 100 global rounds in this experiment.

According to Figure 13 and Figure 14, the DPOT trigger does not change drastically over rounds; instead, it develops gradually and coherently. Since the DPOT trigger is optimized based on the global model’s parameters, and the global model is in turn influenced by malicious model updates backdoored by the DPOT trigger, the DPOT trigger and the global model form a Markov chain. During training, as the global model evolves coherently and gradually, the states of the DPOT trigger evolve as well in the same pattern.

Global model’s accuracy on main/backdoor tasks

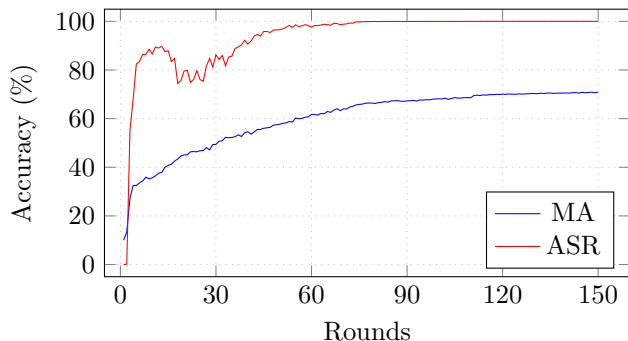


Figure 11: Global model’s accuracy in experiment of getting trigger screenshots in Figure 13. (CIFAR10, ResNet18)

Global model’s accuracy on main/backdoor tasks

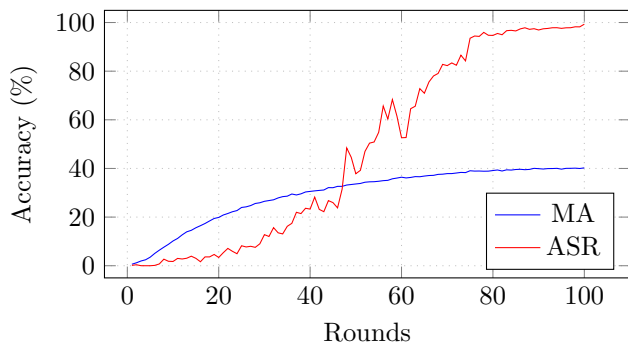


Figure 12: Global model’s accuracy in experiment of getting trigger screenshots in Figure 14. (Tiny ImageNet, VGG11)

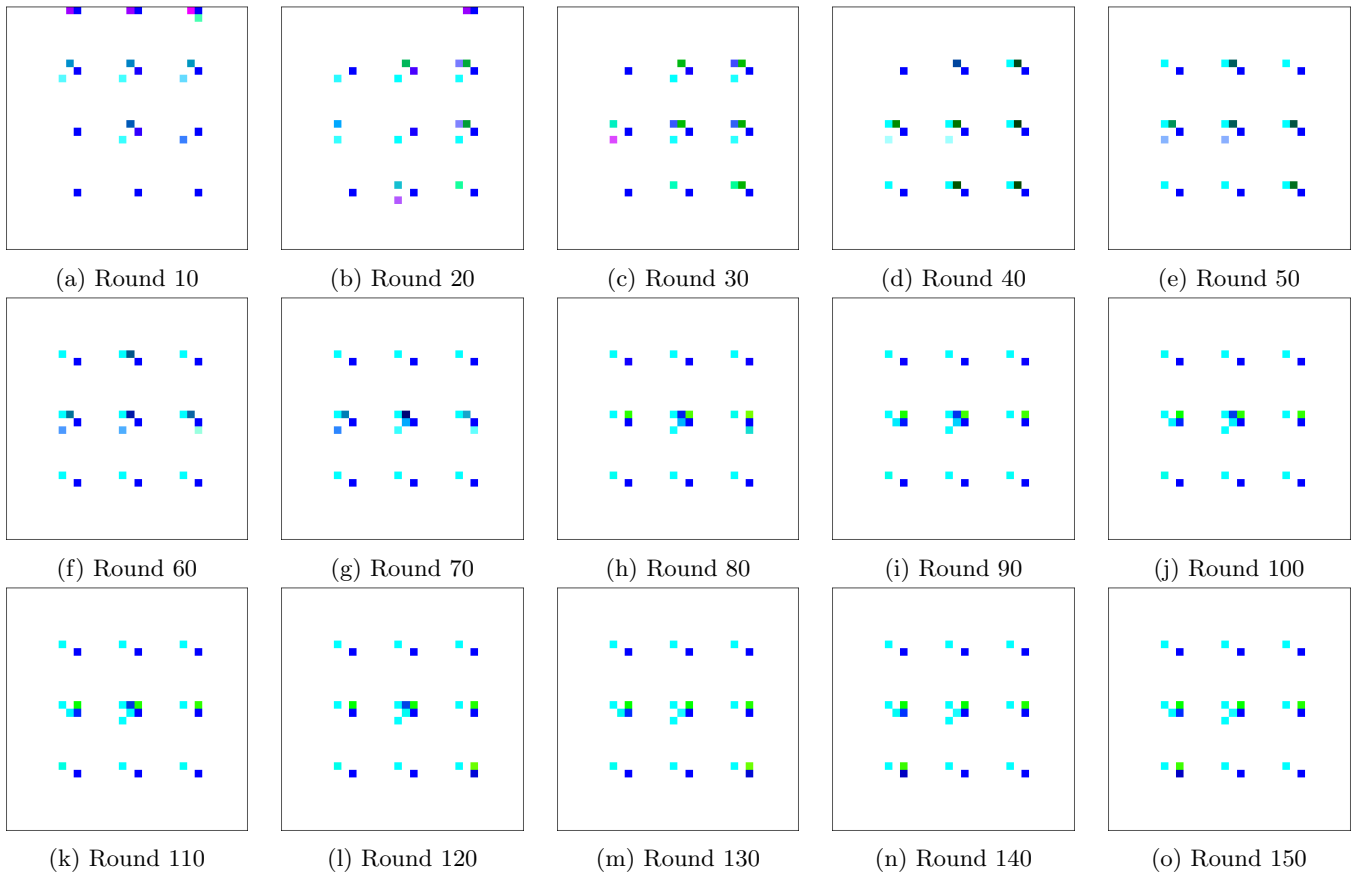


Figure 13: (CIFAR10, ResNet18) DPOT triggers on different rounds.

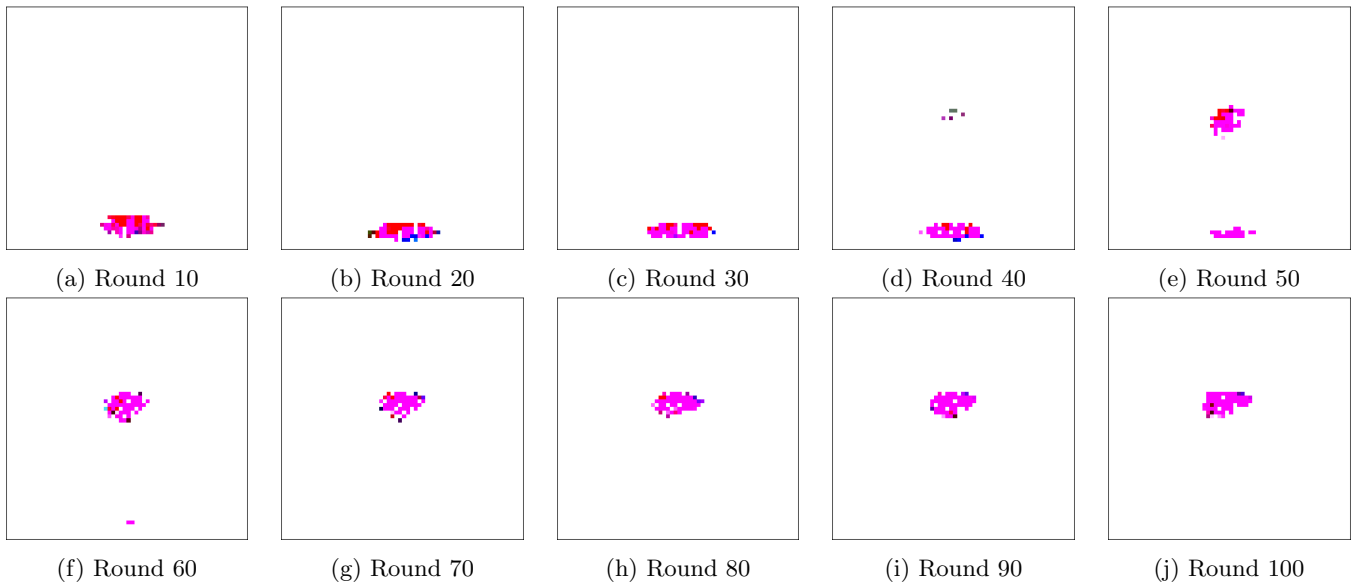


Figure 14: (Tiny ImageNet, VGG11) DPOT triggers on different rounds.

E Evaluation of DPOT attack against Flip [45]

Flip [45] is a client-side defense strategy where benign clients perform trigger inversion and adversarial training using their local data to recover the global model from backdoors. In this section, we evaluate the effectiveness of the DPOT attack against the Flip defense. We implemented the DPOT attack by modifying the data preparation approach in Flip’s open-source project, replacing it with the method used in this work, and injecting our data-poisoning algorithms into a subset of clients. Additionally, as DPOT is a pure data-poisoning attack, we removed any additional steps in their project specified to malicious clients but not existed in benign clients’ training, to ensure consistency between malicious clients and benign clients in FL training. We selected Fashion MNIST as the main-task dataset for our evaluation and directly adopted Flip’s default experiment settings provided in their project - the total number of clients was 100 and 4% of them were malicious clients; the aggregation rule was set to FedAvg; the global model’s parameters were initialized by a pre-trained state. The size of DPOT trigger was set to 64, consistent with our default attacking settings.

We compared the performance of the DPOT attack under two attack patterns provided by Flip’s project: 1) **Single shot**: Each of the 4 malicious clients conducts a one-time attack at the beginning of training. 2) **Continuous**: All 4 malicious clients continuously execute the attack algorithms in every round during training.

Figure 15 shows the performance of the DPOT attack on an FL system using Flip as its defense, measured by the Attack Success Rate (ASR). In the single-shot attack pattern, DPOT maintains a stable ASR of around 15% across all training rounds, exceeding the random guess accuracy of 10% for the 10-class dataset. In the continuous attack pattern, DPOT achieves a significant ASR, peaking at 80.03% during training and stabilizing around 40%, which is higher than the single-shot pattern. These results indicate that Flip is vulnerable to optimized triggers with varying appearances across different rounds, because recovering from backdoors is an after-effect strategy which is unable to stop new and distinct backdoors from injecting into the model.

Figure 16 illustrates the global model’s performance on the main task data when using Flip as a defense while under DPOT attack. We observed that employing Flip reduces the global model’s main-task performance compared to not using it. In our baseline experiment on Fashion MNIST, with the same data distribution and aggregation rule (FedAvg), the model achieved an 86.7% MA. However, Flip’s global model achieved only 82.8% MA at its best by the end, even with pre-trained model

initialization. Additionally, under continuous attack by the DPOT trigger, the global model’s MA further declined compared to the less frequent attack pattern. This raises concerns about Flip’s ability to maintain stable and normal performance on the main task while effectively defending against attacks.

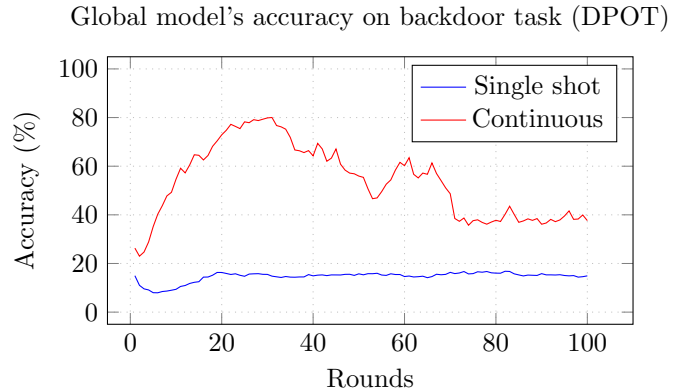


Figure 15: Global model’s Attack Success Rate under DPOT attack when employed Flip as defense strategy. (Fashion MNIST)

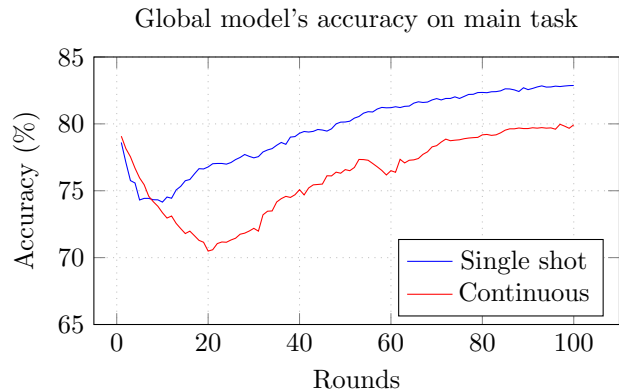


Figure 16: Global model’s Main-task Accuracy under DPOT attack when employed Flip as defense strategy. (Fashion MNIST)

F Evaluation of DPOT attack against FRL [25]

FRL [25] is a defense strategy where the server sparsifies the value space of model updates, allowing clients to vote on the most effective model updates based on their local data. The server then aggregates only the accepted votes while rejecting outliers to construct the global model. In this section, we evaluate the effectiveness of the DPOT attack against the FRL defense. Similar to the experiment on Flip, we implemented our attack on FRL’s open-source project by injecting our data-

poisoning algorithms into a portion of clients’ execution and removing any inconsistent steps that distinguished malicious clients from benign ones during training. We used FRL’s default settings, in which only 2% of clients were malicious, and tested our attack on the CIFAR10 dataset as the main training task.

Table 7 presents the performance results of the DPOT attack on an FL system employing FRL as the defense method. The ASR of DPOT (92.5%) is significantly higher than that of other backdoor attack approaches tested and discussed in FRL’s paper. This indicates that FRL, which relies on analyzing clients’ model updates, is vulnerable to our attack. The evaluation results also demonstrate that the DPOT attack is more advanced than backdoor attacks with static objectives when targeting the FRL defense strategy.

Attacks	ASR
Semantic backdoor attacks	49.2
Artificial backdoor attacks	0
Edge-Case backdoor attacks	64.6
DPOT backdoor attacks	92.5

Table 7: Comparison results on CIFAR10.

G Effects of the scaling-based model poisoning techniques on attacks

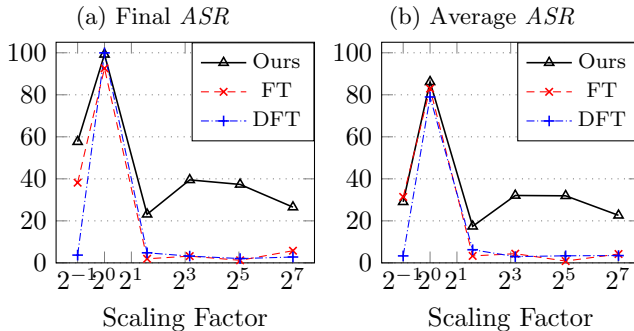


Figure 17: Comparison results of different attacks when employing the scaling-based model poisoning technique to undermine FLAME defense (implemented on the FEMNIST dataset).

In this section, we removed the TEEs assumption and conducted experiments to examine the effects of employing scaling-based model poisoning techniques on the attack performance of DPOT, FT, and DFT. By incorporating the model poisoning technique, our implementation of FT and DFT attacks aligns more closely with the attack strategies introduced in state-of-the-art backdoor attacks on FL [1, 39].

Our experiments were designed within an FL system utilizing FLAME as its aggregation rule and FEMNIST dataset as its main training task. We adjusted the scaling factors, used to scale malicious clients’ model updates, to be 0.5, 1, 3, 9, 33, and 129 respectively. Figures 17a and 17b illustrate the results of Final ASR and Avg ASR of various attacks in response to different scaling factors.

We observed that when the scaling factor is 1, all DPOT, FT, and DFT attacks exhibit comparable and high ASR against FLAME defense. However, as the scaling factor increases, FLAME demonstrates robust defense performance, significantly reducing the ASR of every attack pipeline. Despite this mitigation, DPOT shows greater resilience in attack effectiveness compared to FT and DFT. The optimized trigger generated by our algorithms retains intrinsic attack effects on the global model even without successful data-poisoning techniques. When the scaling factor is reduced to 0.5, malicious model updates are expected to be stealthier, yet their contributions to the aggregated global model are also mitigated, resulting in reduced ASR for all attacks compared to when the scaling factor is 1.

H Main-task Accuracy Results

Table 8 lists the Main-task Accuracy of each experiment in getting results in Figure 5. Table 8 demonstrates that for different datasets used as the main tasks, global models under various attacks maintained a comparable level of Main-task Accuracy to the baselines with no attacks (“None”), indicating that all types of backdoor attacks successfully achieved their stealthiness goals.

Table 9 lists the global model’s Main-task Accuracy of each experiment in getting results in Table 5. Table 5 evaluates the impact of different malicious client ratios on the attack effectiveness of various attacks when using the CIFAR10 as the main-task dataset. Table 9 demonstrates that the performance of global models on Main-task data is not affected by changes in the malicious client ratio, indicating that the stealthiness goals of all backdoor attacks were achieved. “None” represents the baseline MA results with no attack present during FL training.

Table 10 lists the global model’s Main-task Accuracy of each experiment in getting results in Table 6. Table 6 evaluates the impact of different trigger sizes on the attack effectiveness of various attacks when using the CIFAR10 as the main-task dataset. Table 10 demonstrates that the performance of global models on Main-task data is not affected by changes in the trigger sizes, indicating that the stealthiness goals of all backdoor attacks were achieved. “None” represents the baseline MA results with no attack present during FL training.

MA	Tiny ImageNet				Fashion MNIST				FEMNIST				CIFAR10			
	None	Ours	FT	DFT	None	Ours	FT	DFT	None	Ours	FT	DFT	None	Ours	FT	DFT
FedAvg	43.9	43.5	43.0	43.3	86.7	87.3	86.7	86.8	82.2	81.4	83.3	82.3	70.3	70.7	70.4	71.4
Median	40.6	40.2	40.6	38.6	86.0	85.8	86.6	86.3	80.4	81.5	79.8	79.9	70.2	69.1	69.8	69.7
Trimmed Mean	40.8	40.4	40.1	40.6	86.4	85.8	86.4	86.3	80.2	81.7	81.3	81.2	69.4	70.4	70.2	70.8
RobustLR	44.1	42.7	42.9	43.2	86.5	86.8	86.6	86.9	81.8	82.5	81.9	82.6	70.4	70.1	70.3	70.5
RFA	43.6	43.0	43.0	43.0	86.4	86.0	87.1	87.1	83.0	80.7	81.0	80.8	70.4	70.7	70.3	70.8
FLAIR	43.6	42.6	41.8	42.1	86.1	84.9	85.2	84.4	81.5	80.7	80.6	79.7	70.3	70.6	71.0	70.4
FLCert	40.3	40.2	39.7	39.7	86.2	85.9	86.0	86.8	81.3	80.9	81.5	81.0	69.6	70.0	69.8	70.4
FLAME	29.9	28.7	29.2	28.9	86.4	86.4	86.4	86.7	81.8	80.2	80.7	81.0	70.1	70.3	70.9	70.9
FoolsGold	43.1	43.2	43.5	43.2	86.6	87.1	86.8	87.3	83.4	82.7	83.0	81.8	70.4	71.0	71.2	71.7
Multi-Krum	30.7	27.7	27.7	26.4	86.2	85.9	86.0	87.0	79.9	80.4	79.6	80.2	61.4	63.0	63.2	60.8

Table 8: The Main-task Accuracy (MA) of global models in getting representative results in Figure 5. "None" represents no attack existing in the FL training.

MCR		0.05			0.1			0.2			0.3		
		None	Ours	FT	DFT	Ours	FT	DFT	Ours	FT	DFT	Ours	FT
FedAvg	70.3	70.66	70.37	71.37	70.03	71.04	70.13	69.9	70.39	71.18	70.25	70.69	70.24
Median	70.21	69.06	69.76	69.71	69.32	69.17	70.12	68.23	69.05	68.87	68.49	68.47	67.82
Trimmed Mean	69.43	70.42	70.24	70.84	69.9	69.17	69.78	69.33	69.19	69.8	69.23	68.83	68.02
RobustLR	70.35	70.10	70.35	70.48	70.58	70.42	69.90	70.31	70.56	70.43	70.05	69.11	69.22
RFA	70.42	70.69	70.27	70.77	70.35	70.44	70.16	70.72	70.33	69.56	70.09	69.72	69.37
FLAIR	70.25	70.62	71.04	70.42	69.80	71.45	70.89	71.85	71.20	71.16	71.26	69.74	70.99
FLCert	69.6	69.95	69.76	70.42	69.44	69.44	69.45	69.28	69.25	69.73	68.54	69.06	68.24
FLAME	70.14	70.28	70.93	70.85	69.62	70.87	71.01	70.71	70.4	70.58	69.19	71.45	70.52
FoolsGold	70.42	71.02	71.19	71.68	70.71	71.32	71.27	70.45	70.38	70.82	70.12	69.97	69.97
Multi-Krum	61.38	62.98	63.16	60.80	61.44	62.89	62.09	59.38	61.26	63.70	60.28	64.02	62.96

Table 9: The Main-task Accuracy (MA) of global models under different attacks at varying malicious client ratios. (CIFAR10).

Trigger Size		9			25			49			100		
		None	Ours	FT	DFT	Ours	FT	DFT	Ours	FT	DFT	Ours	FT
FedAvg	70.3	70.88	70.72	71.25	70.66	70.37	71.37	70.77	71.35	70.94	69.92	70.71	71.15
Median	70.21	68.31	70.04	68.69	69.06	69.76	69.71	69.95	70.54	70.56	69.88	70.30	70.86
Trimmed Mean	69.43	69.75	70.13	70.19	70.42	70.24	70.84	69.42	70.17	69.79	69.67	70.26	70.68
RobustLR	70.35	70.48	70.95	69.48	70.10	70.35	70.48	70.79	70.08	70.27	70.39	69.73	69.86
RFA	70.42	70.45	70.16	71.00	70.69	70.27	70.77	70.56	70.19	70.62	70.52	69.22	70.77
FLAIR	70.25	70.79	70.67	70.58	70.62	71.04	70.42	70.84	69.96	71.03	71.17	70.65	70.28
FLCert	69.6	69.88	69.64	69.87	69.95	69.76	70.42	67.77	69.83	70.08	68.81	70.81	70.41
FLAME	70.14	70.07	71.24	70.19	70.28	70.93	70.85	69.87	71.20	70.68	67.24	71.06	70.75
FoolsGold	70.42	70.4	72.1	70.09	71.02	71.19	71.68	70.66	70.75	71.38	69.84	71.06	71.64
Multi-Krum	61.38	62.86	64.65	58.90	62.98	63.16	60.80	58.23	60.16	64.04	63.03	61.64	63.33

Table 10: The Main-task Accuracy (MA) of global models under different attacks with varying trigger sizes. (CIFAR10).